I have contributed equally with my team partner in this assignment

Melissa King Rebecca Napolitano

Proposal for Diagnostic Monitoring of the South Wall of the Nave at La Vieja Misión

San Antonio, Texas

December 17, 2018

Rebecca Napolitano

PhD Candidate in Civil and Environmental Engineering at Princeton University

Melissa King

Graduate Fellow in Preventive Conservation at the Winterthur/University of Delaware Program in Art Conservation

TABLE OF CONTENTS

1. EXECUTIVE SUMMARY

La Vieja Misión and the surrounding sites have been at the center of attention from its stewards in Texas lately. Nearing its tricentennial, the site has been designated as a national historic landmark and a world heritage site. Since La Vieja Misión is of great significance and value in not only Texas but now on a global scale, a comprehensive assessment of the building and its needs for interventive and preventive conservation have been carried out.

With regards to the results of this assessment, there are evident conservation issues that need to be addressed. Preliminary assessment of the stone masonry walls has determined that subflorescence of salts along with disaggregation and erosion of stone are the dominant modes of stone degradation at the church. As the stakeholders are aware, the current state of deterioration at La Vieja Misión is not sustainable.

Our proposed solution is to use nondestructive testing in conjunction with in-situ monitoring to ascertain the predominant drivers of deterioration in La Vieja Misión. Water-related problems are the most prevalent causes of damage and degradation in cultural heritage and historic buildings, and we believe it to be a major contributor to the deterioration of La Vieja Misión. In particular, we hypothesize that the water-related problems could be due to cycling of the interior and/or exterior relative humidity, rain (including near surface soil moisture), and subgrade moisture sources.

As a preliminary evaluation, we propose to monitor the moisture content within the south wall of the nave. This wall has been selected as it as it faces more climatic factors due to its southern exposure. Specifically, we plan to integrate detailed systems diagrams of the moisture and deterioration sources to the wall with information about the site's historical background, previous structural changes, and prior climate data to optimize the types of sensors which are instrumented on the wall and the modes of data analysis which are utilized.

With this proposed diagnostic and monitoring plan, we aim to isolate the sources of moisture to different regions on the south wall to understand which predominant mode of moisture flow is the most detrimental to the structure. Quantitative evidence for the impacts of each moisture mode will serve as actionable information which can be used by the stewards of La Vieja Misión in future interventive and preventive conservation. This proposal outlines in more detail how we will carry out this plan, and what you can expect along the way.

You should consider King and Napolitano Conservators because we are proud to be interdisciplinary experts in building diagnostics and monitoring. That means we are among an elite group of conservators who have been trained in not only building diagnostics and monitoring, but also preventive conservation and structural engineering. This makes us uniquely

qualified for this project as it has been outlined in the call for proposals that the site is in need of not only interventive conservation, but also preventive conservation.

Thank you for your time and consideration. We appreciate the opportunity to work with you on this project. Please call us if you any questions or concerns.

Sincerely,

King and Napolitano Conservators

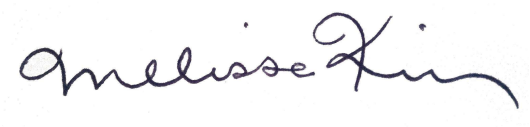

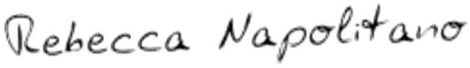

Melissa King

Rebecca Napolitano

2. BACKGROUND AND OVERVIEW OF THE BUILDING

2.1 Structural History

Construction on La Vieja Misión was started in 1724.[1] The ensemble of missions in San Antonio is one of the most intact examples of Spain's attempt to evangelize and colonize the northern frontier of New Spain.[2] La Vieja Misión is the most northern of the missions and is located in an urban setting[3]. The mission complex consisted of the chapel, a presidio, a granary, a convent, barracks for the soldiers, rooms for the natives, a hospital and a plaza (for maps see Appendix I).[4] The construction of La Vieja Misión finished in 1757 and included twin towers, vaulted roofs, and a multi-colored dome; however, the dome and some of the vaults collapsed before 1762.[5] By 1793, the mission was secularized and remained within military occupancy with some repairs made in the 1820's until the siege of 1836. During the siege, alterations were made to the walls in preparation for the battle and following the battle the chapel was left in ruins.[6] From 1848 to 1849, major improvements were made to the building, including the rebuilding of the parapet on the West façade, the creation of windows in the original stone wall, the completion of a roof, and the front gable was given its current profile.[7] In 1861, a fire destroyed the chapel's roof.[8] In 1920 a new timber roof was constructed that was replaced again in 1934 with reinforced concrete vaults covered with lead[9]. The chapel has been without a roof for over 60% of the time since it was built (see Figure 1). For more information about the history of the site, see Appendix II. For historical images of the structure during different periods, see Appendix III.

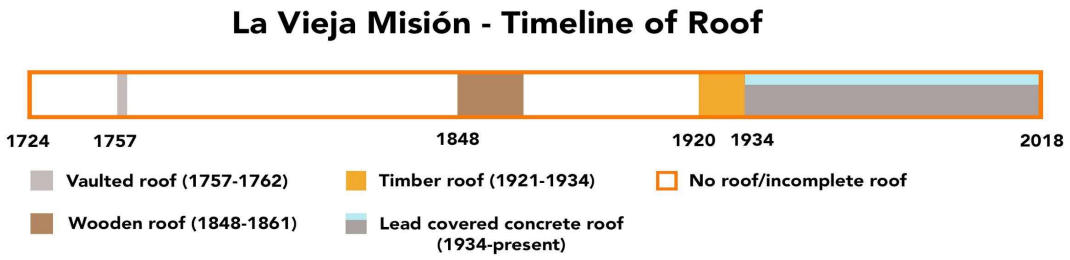

Figure 1: Timeline that shows the history of roof construction

[1] "San Antonio de Valero Mission," Texas State Historical Association, accessed November 19, 2018, https://tshaonline.org/handbook/online/articles/uqs08

[2] "San Antonio Missions," UNESCO Nomination to the World Heritage List by the United States of America, self published, 2014, 4

[3] "San Antonio Missions," UNESCO, 30

[4] Library of Congress, Prints & Photographs Division, HABS, 1961

[5] HABS, 1961

[6] "San Antonio de Valero Mission," Texas State Historical Association, accessed November 19, 2018, https://tshaonline.org/handbook/online/articles/uqs08

[7] HABS, 1961

[8] "San Antonio de Valero Mission," Texas State Historical Association, accessed November 19, 2018, https://tshaonline.org/handbook/online/articles/uqs08

[9] HABS, 1961

2.2 Location

La Vieja Misión is located in San Antonio, Texas. While on high ground, the mission is still located less than 500 meters East of the San Antonio River. The grounds that surround the Mission are landscaped with live oak trees, well-kept lawns, and flowering bushes and plants, which require regular irrigation[10]. These types of oak trees are known to shed their leaves from March through early May of every year.[11] For the first quarter of the 18th century, the ground where the church is was used as a burial ground.[12] As evidenced by Sanborn drawings (see Figure 2), La Vieja Misión was within close proximity to many mechanic shops and even a tire factory, which could be responsible for sulfur pollutants in the air (sulfur dioxide and reduced sulfur compounds).

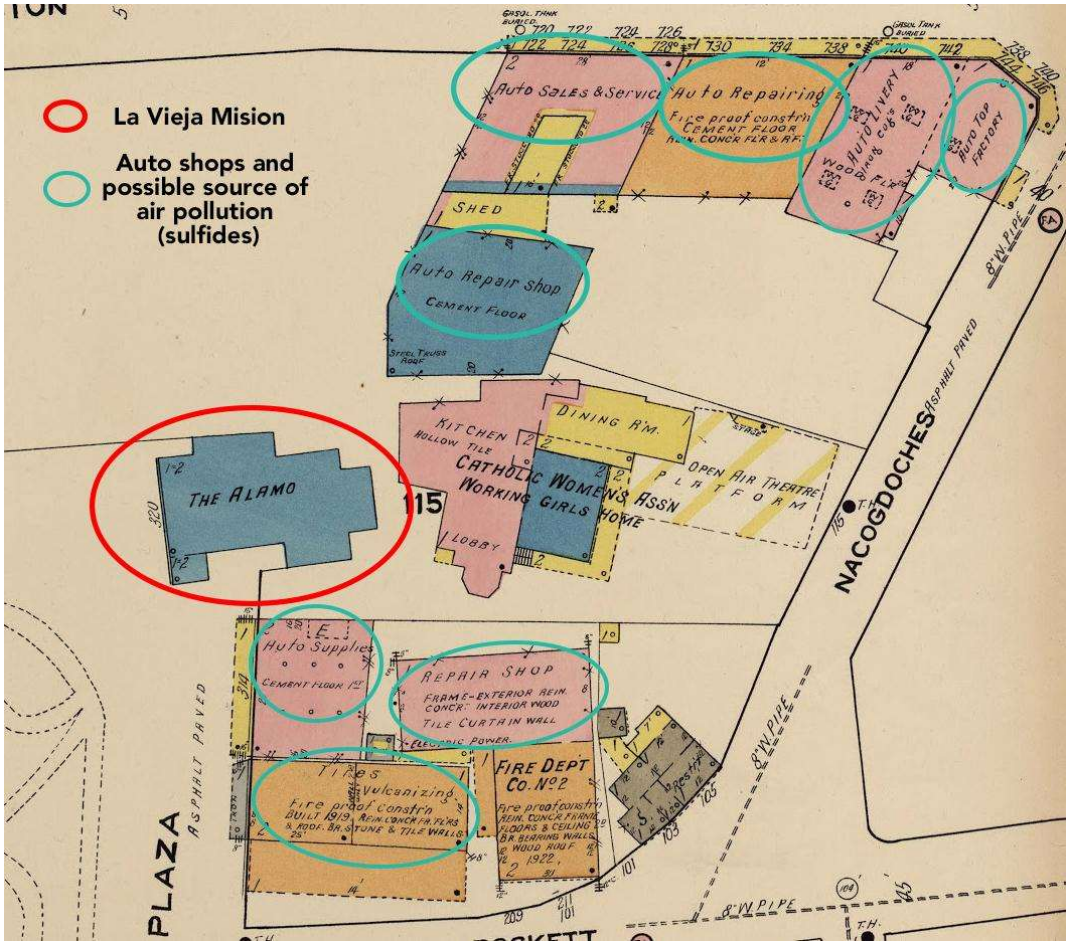

Figure 2. 1922 Sanborn drawing that shows the proximity of La Vieja Misión to auto shops and vulcanizing factories that could serve as a source of sulfur pollutants.

[10] "San Antonio Missions," UNESCO, 86

[11] "Annual Texas Live Oak Leaf Drop," Texas Plant Disease Diagnostic Lab, Texas A&M Agrilife Extension, accessed November 30, 2018, https://plantclinic.tamu.edu/2011/03/30/annual-texas-live-oak-leaf-drop/

[12] Michael Henry, Class Instructions for Building Diagnostics, University of Pennsylvania, October 12, 2018.

2.3 Climate and Extreme Weather Events

Historically, San Antonio's weather is humid and subtropical.[13] The summer experiences average high dry bulb temperatures in the upper 90's °F, and winters have average low dry bulb temperatures in the upper 30's °F (see Appendix IV). According to the National Weather Service Report for San Antonio, the winter can have cool to cold nights, and every two or three years the temperatures may allow for snow, sleet, or freezing rain. The city is prone to flooding, and typically experiences the greatest amount of rain in the Spring and Fall. Additionally, the area has been prone to occasional earthquakes and hurricanes as can be seen in Figure 3.

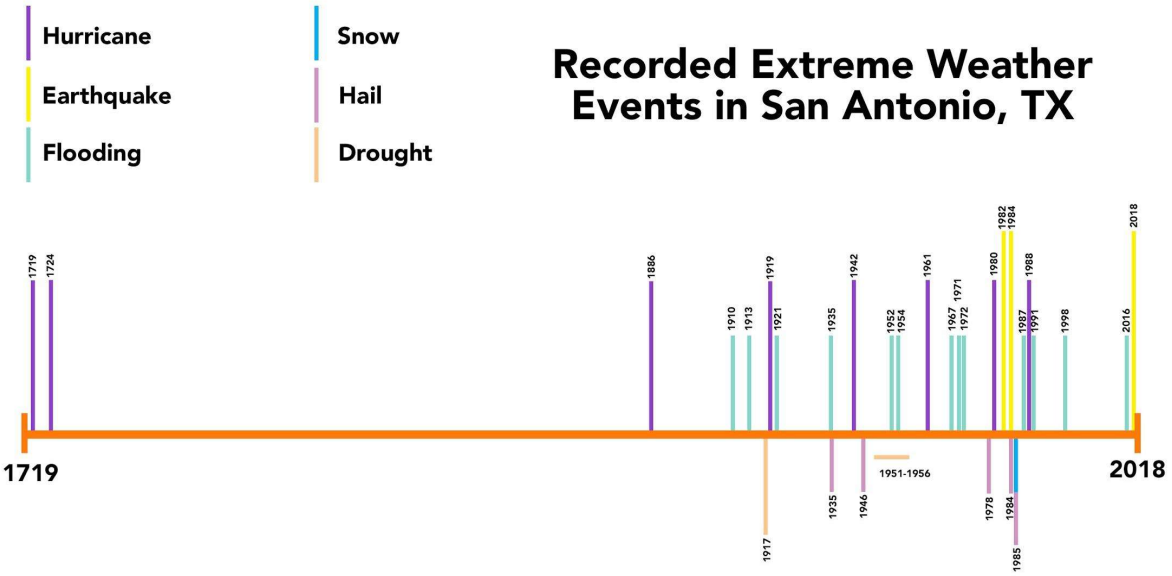

Figure 3. Timeline of recorded extreme weather events in San Antonio, Texas.

2.4 Contemporary Use

For over 140 years the building has been used as a museum and in recent years has seen more than 2 million visitors a year.[14] In 2015, the building was added as a World Heritage Site through the United Nations Educational, Scientific, and Cultural Organization. Due to the high numbers of visitors and the need for human comfort, air conditioning is employed in the summer months.[15] It has also been noted that the entrance and exits to the museum are consistently open to allow for the flow of visitors.[16]

[13] "San Antonio Missions," UNESCO, 6
[14] "San Antonio Missions," UNESCO, 240
[15] Michael Henry, Class Instructions for Building Diagnostics, University of Pennsylvania, October 12, 2018.
[16] Michael Henry, October 26, 2018.

2.5 The South Wall of the Chapel

The wall for proposed monitoring is located on the South side of the chapel's nave. There is an assumed footing that is composed of unknown materials but is likely similar to the rest of the wall.[17] The stones of the walls were assessed by a stone conservator and four types of limestones were identified (see Appendix V). The interior of the wall is covered in lime plaster.[18] The roof is made from reinforced concrete with a lead coating.[19] Additionally, there is a coating of mastic on top of the concrete parapet that does not extend over the edge.[20] Drainage for the roof is from spaced out canales that exit through the side of the wall. The interior floor of the church that abuts the south wall is composed of waxed concrete slabs with an asphaltic membrane that was installed to prevent salt efflorescence.[21]

[17] Michael Henry, October 19, 2018.
[18] HABS, 1961
[19] Michael Henry, October 5, 2018.
[20] Michael Henry, October 19, 2018.
[21] Michael Henry, October 26, 2018.

3. DESCRIPTION OF CONDITION/PERFORMANCE PROBLEM

3.1 Overall Condition of the Wall

The plaster is falling off the bottom half of the interior side of the south wall (Figure 4). According to a report generated by a stone conservator, the stone is actively deteriorating through delamination, and it is visibly recessed below the mortar.[22] On the exterior of the wall, there is a dark staining along the concrete cap of the pilaster, which could be a result of biological growth and/or dark gypsum.

Figure 4: (left) Evidence of rising damp and loss of plaster on the interior wall. (right) Deterioration of stone through delamination

3.2 Presence of Soluble Salts

The loss of plaster on the interior wall is possibly the result of subflorescence, which is caused by soluble salts (sulphates, nitrates, and chlorides) from the ground being transported through the wall as ions in water and recrystallizing beneath the plaster surface upon drying.[23] The salts could be recrystallizing behind the plaster (subfluorescence) causing it to separate from the stone and mortar or the salts could be forming within the plaster causing the plaster to disintegrate. When considering the location of the plaster damage, it is feasible that the losses are correlated to the rising damp from water in the soil. The recrystallization can cause internal fractures within the matrix of the stone and mortar as well. The caretakers of the chapel installed an asphaltum barrier below the concrete slabs of the interior floor and waxed the surface of the floor as an attempt to prevent soluble salts from efflorescing on the floor of the chapel (Henry, pers. comm.). These barriers could result in an increase in salts within the wall as rising damp below the floor is forced to find another way around the sealed surface of the floor.

[22] Michael Henry, Class Instructions for Building Diagnostics, University of Pennsylvania, October 5, 2018.
[23] Rosa Espinosa, Lutz Franke, and Gernod Deckelmann, "Predicting Efflorescence and Subflorescences of Salts," MRS Proceedings 1047 (January 2007), https://doi.org/10.1557/PROC-1047-Y04-03.

Because different soluble salts crystallize and deliquesce at specific relative humidities, changes in relative humidity can be directly responsible for salt crystallization damage.[24]

3.3 Physical Deterioration of the Stone and Mortar

The north wall is composed of three different types of limestones (see Appendix V). Limestones are composed of various minerals of calcium salts, which are formed through sedimentary deposition. In the formation of sedimentary rocks, clay depositions can separate layers of calcium mineral formations, which is what can be seen within the highly prevalent grey greenstone.[25] The variety of limestones in the wall have different interactions with water. The hydrophilic tendency of clay particles will attract water when the stone is wet causing internal expansions within the layers of the stone. These expanding clay layers within the stone are likely the cause of the visible delamination and the cleaving of the stone surface (Figure 5). The stone appears to be sacrificial to the mortar, which suggests a higher compressive strength (SOURCE). Due to the time period, there is a possibility that the mortar was created with the use of pozzolana, which would be responsible for the added strength.[26] The various materials of the stones and mortar represent different porosities and equilibrium moisture contents. The composite materials also contain various coefficients of thermal expansions, which can be a cause of deterioration of the stone when the South-facing wall is heated from the sun.[27]

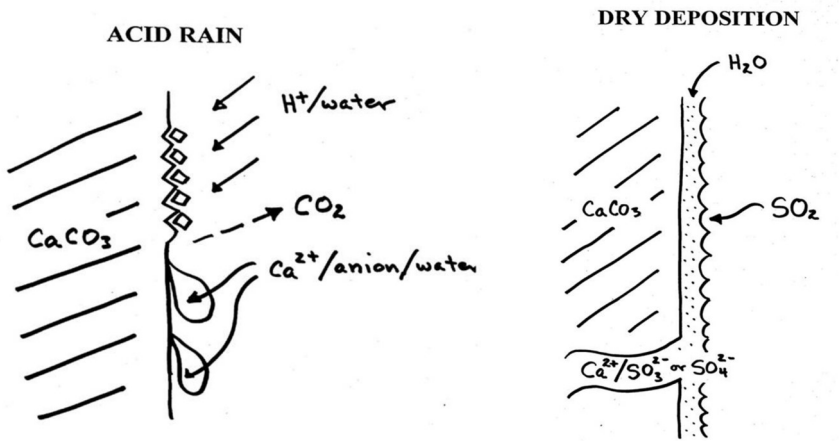

Figure 5. Diagrams exhibiting the various formation of gypsum on a carbonate-based stone [28]

[24] Changgeng Peng and Chak K Chan, "The Water Cycles of Water-Soluble Organic Salts of Atmospheric Importance," *Atmospheric Environment* 35, no. 7 (January 1, 2001): 1183–92, https://doi.org/10.1016/S1352-2310(00)00426-X.

[25] Michael Henry, October 5, 2018.

[26] David S. Watt, *Building Pathology* (Oxford: Blackwell Publishing, Ltd, 2007), 63.

[27] Watt, *Building Pathology*, 125.

[28] George Wheeler, stone conservation lecture, Winterthur/University of Delaware Program in Art Conservation, March 5, 2018.

3.4 Black Staining on the Exterior Wall

Excess dampness, high temperatures, bioaerosols, and the mineral salts in the walls create the perfect combination for the colonization of bacteria and fungus.[29] These organisms can produce metabolic acidic products and enzymes that can cause deterioration to the walls.[30] Many fungal and bacteria species contain pigments, which might result in the dark coloring seen on the side of the building.[31] Due to the calcium-based nature of the concrete and limestone, the wall is susceptible to the formation of gypsum. Gypsum can be formed from acid rain combined with the presence of sulphates in the air (Figure 5).[32] Due to the urban setting and historic proximity of auto mechanic shops, there is a high likelihood of current and past sulfur pollution in the air. When sulphate salts encounter cement-based mortars and concrete, ettrengite mineral can be formed. Ettengrite is highly hygroscopic, which can lead to expansion and ultimate deterioration of the cement.[33]

3.5 Performance of the Roof

In 2012, contractors were hired to repair the roof's structural deficiencies and prevent further moisture infiltration (Figure 6).[34] It is unclear how this was repaired, but it is possible that there may have been cracks as a result of the lack of expansion joints.[35] The lead roof will expand and contract in hot and cold weather and if there is nowhere for the lead to move it can cause splitting. It is also possible that there could be cracking in the concrete due to its poor working properties under tension. Mastic is coating the upper surface of the concrete parapets but to avoid a visual disturbance, it does not extend over the corners, which provides access points for rain water into the wall. Since the roof has a lead coating, it is a great conductor of heat and may an impact interior temperature. The radiation of heat from the roof is evidenced in the poor performance of the HVAC condensers on the roof that may be attributed to vapor lock from the heat or overflow from rain water.[36]

---

[29] Watt, *Building Pathology*, 131.

[30] Ibid

[31] Florian, Mary-Lou E. *Fungal Facts: Solving Fungal Problems in Heritage Collections*. London: Archetype Publications, 2004. 8

[32] George Wheeler, stone conservation lecture, Winterthur/University of Delaware Program in Art Conservation, March 5, 2018.

[33] Watt, *Building Pathology*, 123.

[34] "San Antonio Missions," UNESCO Nomination to the World Heritage List by the United States of America, self published, 2014, 236

[35] Michael Henry, October 26, 2018.

[36] Ibid

Figure 6: 2012 repairs of the roof.

3.6 Environmental Controls

Because of the high heat during summer months in Texas and the prioritization of human comfort, the air in the building is conditioned during the summer.[37] As seen in Figure 7, the doorways are not perfectly sealed, and they are also regularly opened because of the Mission's high visitation rates. In the winter, the building is unheated, with air exchange through the doorway.

Figure 7: Image of the nave interior that shows large gaps in the door frame.

[37] Michael Henry, October 19, 2018.

4. THREE SOURCES OF MOISTURE AND THEIR EFFECT ON THE WALL

Moisture penetration of the wall can be caused by vapour in the air, rising damp, and penetrating damp caused by rain. Increased moisture content within the walls can cause an expansion of the volume of the material and conversely shrinkage and cracking upon drying. This volume change is especially a problem for the clay-based stones in the wall and the composite nature of the materials that make up the wall. Other deterioration problems resulting from the presence of water vapour can be internal fractures from the critical salt cycles and the solubilizing and recrystallizing of salts deposited from the rising damp, chemical deterioration, and biodeterioration. An increase in salt levels deposited from rising damp can also reinforce the moisture levels within the wall matrix.[38] Water is the most damaging and widespread cause of degradation and decay in buildings, which is why it is the focus of our evaluation and proposed monitoring.[39]

4.1 Cycling of Interior and/or Exterior Relative Humidity

Relative humidity refers to the ratio of moisture in the air to the total moisture it would contain if it was fully saturated at the same pressure and temperature.[40] If the air does become saturated (100% RH), condensation can form on cold surfaces, and when the dew-point temperature is reached within the thickness of construction, interstitial condensation can form.[41] Since temperature on the inside and outside of the building can vary, especially during the summer months when the building space has conditioned air, there will be a variation in the temperature gradient of the wall. Because the South wall at La Vieja Misión is quite porous, we are most concerned about interstitial condensation and an increased moisture content as a water source and potential contributor to its degradation.

Internally, high relative humidity can be reinforced by water usage in the building as well as rising damp, leaks, spillages, and rain penetration. Other reinforcing feedbacks can be caused by infiltration loads to the building such as open doors, and gaps within door and window frames, which can allow an increased dew point in the space. For more information about flows throughout the system and feedback loops, see the systems diagrams provided in Appendix VI. In the wintertime when the wall is cooled from external temperatures, an increased internal dew point may cause high humidity within the matrix of the wall and potential interstitial condensation. Externally, the relative humidity can be reinforced by rain and varied temperature. Balancing feedbacks in the moisture levels in the wall can be the decrease in relative humidity through the lowering of dew point temperature and increase of temperature within the space.

[38] David S. Watt, *Building Pathology* (Oxford: Blackwell Publishing, Ltd, 2007), 130.
[39] Watt, *Building Pathology*, 114.
[40] Watt, *Building Pathology*, 118.
[41] Ibid

4.2 Rain and Near Surface Soil Moisture

Liquid water can enter the matrix of the wall through wind-driven rain and near surface soil moisture that is retained in upper layers of soil after rain accumulation and local irrigation. This water damage can increase if there are existing cracks and defective joints. Since there is a long history of the building not having a roof (Figure 1) and also because the mastic covering does not extend over the edge of the concrete parapets, it is also possible for rain water to enter into the wall through its top.

Wind speed and direction can reinforce wall dampness if rain and north-blowing wind occur concurrently. In December, January, and February the wind direction is typically blowing north at a rate of 6-14 knots (Appendix IV). The average rain accumulation ranges during these months range 1.5-1.8 inches, which is relatively little. In September, October, and November, San Antonio does experience north-blowing wind, the wind speed averages are lower between 1-5 knots (Appendix IV). These months do have a higher average precipitation rate than the winter months, which could account for some moisture on the wall as a result of wind-driven rain. Of course, there are also singular, extreme weather events that could contribute to damage from this source of moisture, which can also contribute to near surface moisture. The amount of moisture derived from rain splashing directly on the wall from wind can be more adequately determined through the proposed monitoring plan (Section 5). Wind speed and direction can also work as a balancing feedback in wall dampness since they can also increase the rate of drying of the walls.

The canales were created to direct drainage from the roof away from the building, but the discharge area in the ground and pooling from rain directly on the ground and surrounding pavement could also be a potential source for water within the wall. While monitoring of soil moisture directly under the canales has not been proposed in this preliminary investigation, it is recommended for more detailed assessment in the future. As visible in Figure 8, the flood risk for the area of the structure appears to be relatively low, but man-made barriers such as asphalt can increase localized risk of flooding.

Reinforcing and balancing feedbacks for penetrating damp can be determined by the exterior relative humidity (low RH and high RH respectively), since this can affect the drying time of damp soil and water that has collected on the surface of the wall. Another balancing feedback loop for moisture within the wall could be the amount of solar radiation and increased temperature as these can also aid in the evaporation of water. The average incident solar radiation in San Antonio is lowest in the summer months when the rain levels are the highest; however, drying can occur from the higher dry bulb temperatures during these months (see Appendix IV).

Figure 8: Red circle indicates the location of the structure, the green lines indicate risk map streams, blue highlights indicate flood depth (1% annual chance), green highlighted sections indicate 30-year risk of flooding. [42]

4.3 Subgrade Moisture

Water can enter a wall due to capillary forces and osmosis from lower to high salt concentrations.[43] The movement of moisture is highly dependent on the porosity of the wall materials and the presence of any salts. Water entering the wall from subgrade moisture would require absence or failure of a damp-proof course or membrane. The footing of the building is unknown but its age and the evidence of rising damp on the walls suggests there is no effective barrier.

A 1984 soil report suggests that the water table is 17-20 feet below grade.[44] Since the water table is relatively low, it is not expected to be a major contributor to the water damage visible in the wall. However, this will be confirmed or denied through proposed groundwater level monitoring. However, the building has had a history of efflorescence on the floor which has influenced stakeholders to install asphaltum and wax membranes.[45] If rising damp is resulting from subgrade moisture (accumulated either from penetrating rain, groundwater, or both), the barrier in the floor may channel water into the wall through capillary action.

[42] "SARA Risk Map Viewer" FEMA, accessed December 16, 2018, https://sara-tx.maps.arcgis.com/apps/webappviewer/index.html?id=0b13614f13124257bfe589a459ba84fe

[43] Watt, *Building Pathology*, 115.

[44] Raba-Kistner Consultants, INC, *Soil and Groundwater Study Progress Report No. 1 The Alamo Shrine San Antonio, Texas*, technical report (1984).

[45] Michael Henry, October 5, 2018.

4.4 Illustrating potential damage locations for each type of moisture

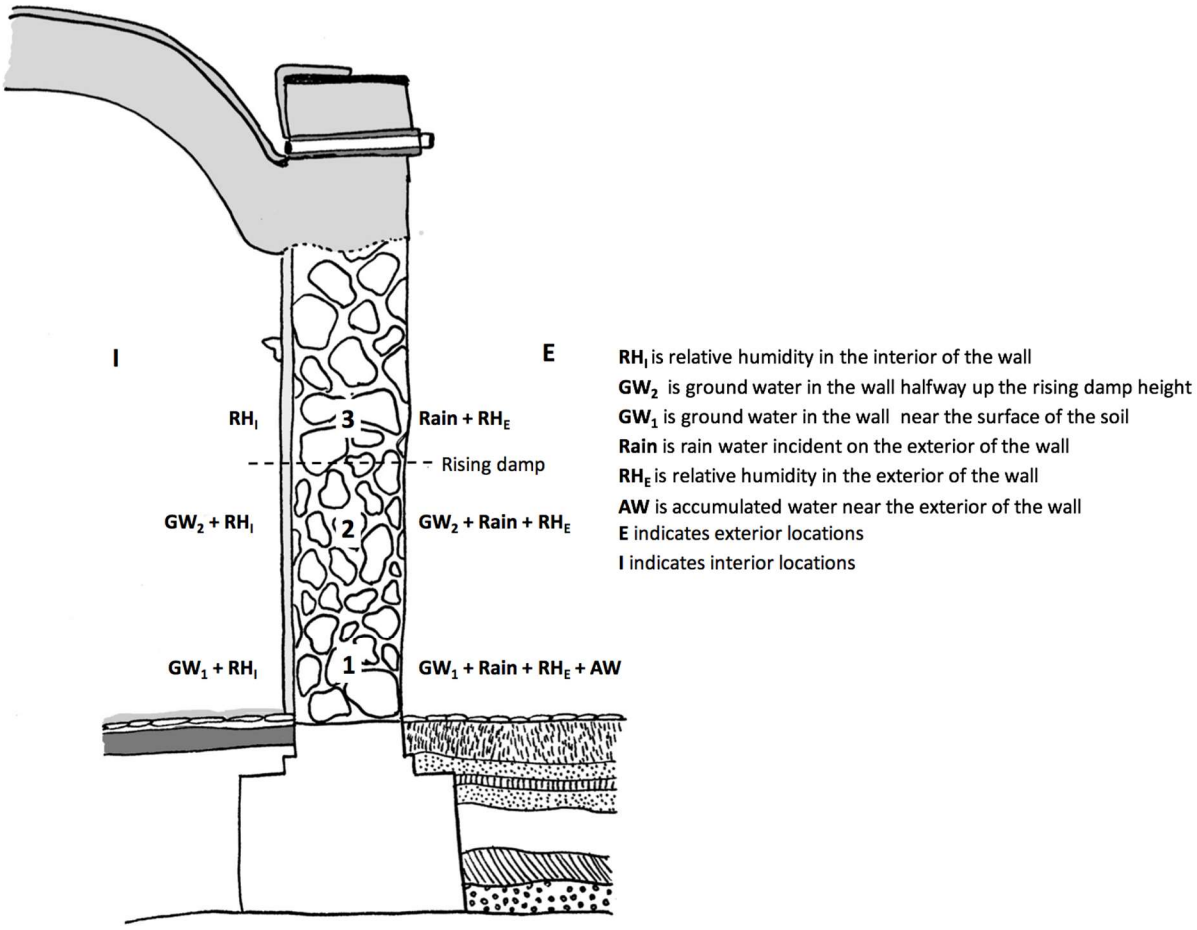

Figure 9: Potential damage locations for each type of moisture

Figure 9 illustrates which of the moisture components affects the different parts of the wall and assumes a no transfer zone in the middle of the wall. 1 is a point along the bottom of the wall (8-11" from the ground), 2 is a point in the middle of the rising damp line, 3 is a point above the rising damp line. The exterior wall at point 1 (E1) is affected by all three sources in the form of groundwater, direct rain, accumulated water along the side of the wall from rain, as well as external relative humidity. While the exterior of the wall at point 2 (E2) is still impacted by the rain and external relative humidity, the effects of groundwater will be lessened as this sensor is higher up on the wall as well as there is not water ponding next to the surface of the wall as there was on the exterior of the wall in position 1 (E1). Since the exterior of the wall in position 3 (E3) is above the line of rising damp, it is only affected by rain and external relative humidity. The interior of the wall in position 1 (I1) is not affected by rain or external humidity. While the effects of accumulated rain water can sometimes be perceived if there is a great enough

difference in height on the two sides[46], there is not a great difference in height here and seepage under the foundations is not accounted for. Therefore, the interior of the wall in position 1 (I1) is only impacted by groundwater levels and interior relative humidity. The interior of the wall in position 2 (I2) has the same actors, however as with the exterior, the effects of groundwater are lessened as the height up the wall increases. The interior of the wall in position 3 (I3), as it is above the line of rising damp, is only affected by the interior relative humidity.

[46] NPTEL, "Seepage in Soils," Soil Mechanics Modules and Lectures, accessed December 16, 2018, https://nptel.ac.in/courses/105103097/25.

5 PROPOSED MONITORING METHODOLOGY

5.1 Introduction to monitorable parameters

The section of the wall shown in Figure 10 will be monitored to understand how the effects of the three sources of moisture discussed in Section 4 can be quantified and compared. This location has been chosen as it is removed from influences of water draining from the canales or water overflowing off the roof of the baptistery as well as it does not include a window. This section of the report will first provide information about what parameters should be monitored, why they are important, and general information about them. Second, information about specific sensors, locations, accuracy, and data analysis/gathering will be discussed. Third, a discussion about the loggers selected and data retrieval will be included. Lastly, methods for data processing will be discussed.

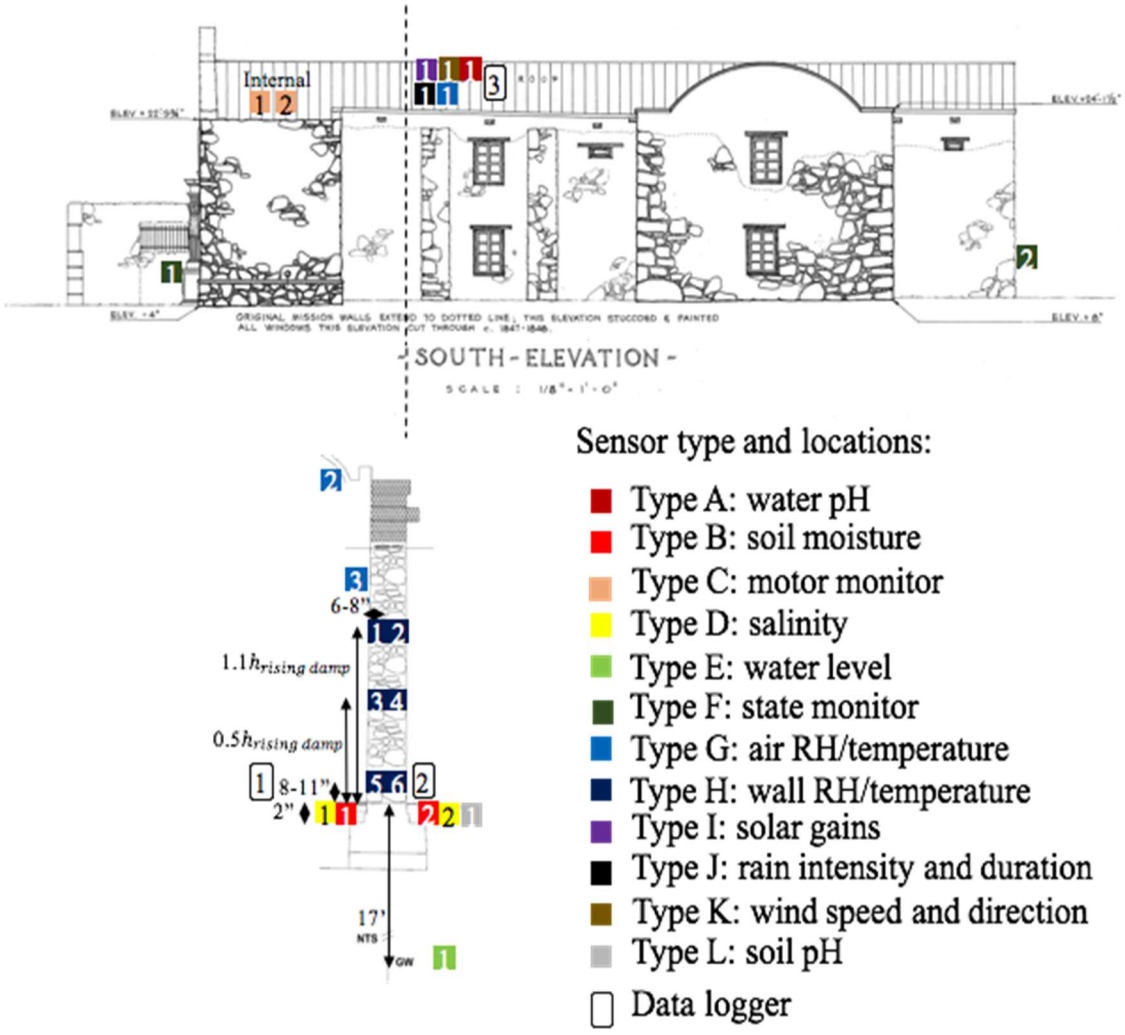

Figure 10: Map indicating the locations of sensors on the south wall on both the interior and exterior. Color indicates typology and the number is incremental within the typology.

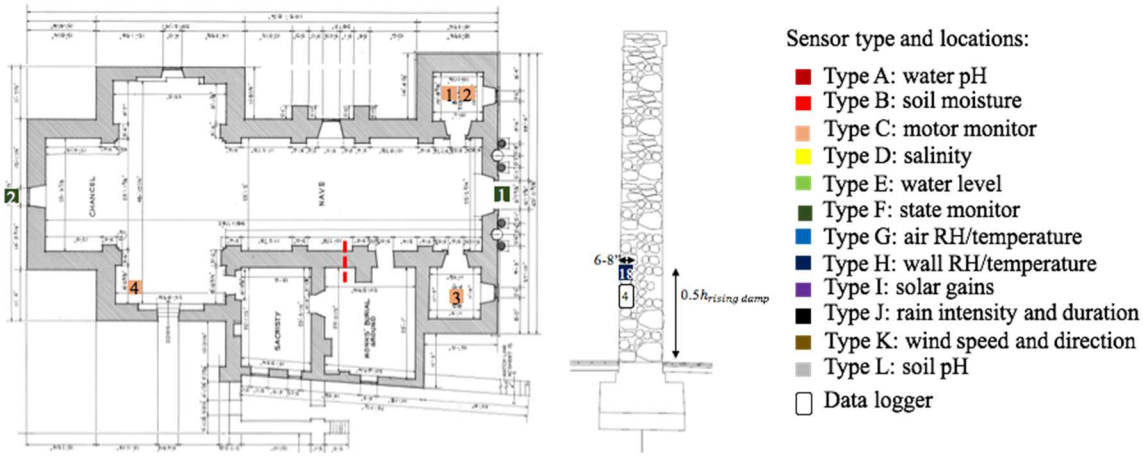

Figure 11: Map indicating the locations of sensors in locations aside from the south wall. Color indicates typology and the number is incremental within the typology.

5.1.1 Monitorable parameters affected by rain (including near surface soil moisture)

To monitor how rain (including near surface soil moisture) would affect the moisture content of the wall, the relative humidity within the wall should be measured. This measurement of relative humidity is directly related to the moisture content and therefore provides a satisfactory and quantifiable point of comparison for the other monitorable parameters. This can be measured near the bottom exterior surface of the wall to see how any accumulations of water near the ground level affect the moisture content of the wall, as well as in an additional, higher section on the exterior of the wall to see the effects of wind-driven rain. Considering a system diagram for only rain and near surface soil moisture sources (see Appendix VI, Figure A.VI.B) in conjunction with the climate data presented in Appendix IV, the monitorable parameters related to moisture are soil moisture content, rain amount, and intensity of rain. Additionally, the monitorable parameters related to drying are solar gains, wind speed, and wind direction.

5.1.2 Monitorable parameters affected by subgrade moisture from the lower aquifer

To monitor how subgrade moisture would affect the moisture content of the wall, again the relative humidity within the wall should be measured. It can be measured halfway up the rising damp ($0.5h_{rising\ damp}$), as well as above the line of rising damp ($1.1h_{rising\ damp}$). The rising damp height can be assessed using infrared thermography in accordance with methodologies outlined in previous literature.[47] [48] The FLIR E53 240 × 180 Advanced Thermal Imaging Camera is recommended for this application as it has an accuracy of 2% of the reading and the temperature range of -4°F to 248°F

[47] Elisabetta Rosina and Nicola Ludwig, "Optimal Thermographic Procedures for Moisture Analysis in Building Materials," Diagnostic Imaging Technologies and Industrial Applications, September 10, 1999, , doi:10.1117/12.361015.

[48] E. Barreira, R.m.s.f. Almeida, and J.m.p.q. Delgado, "Infrared Thermography for Assessing Moisture Related Phenomena in Building Components," Construction and Building Materials 110 (2016): , doi:10.1016/j.conbuildmat.2016.02.026.

firmly covers the range necessary for this application. The groundwater levels should be monitored to see if there is any correlation with the relative humidity in the wall.

5.1.3 Monitorable parameters affected by cycling of the interior and/or exterior relative humidity

To monitor how the cycling of the interior and/or exterior relative humidity would affect the moisture content of the wall, the relative humidity should be measured in both the interior and exterior of the building and in the air both in and outside of the structure. Additionally, it can be measured on an interior wall as a control; for further discussion about the use of a control wall see Section 6.1. In addition to measuring the relative humidity, the number of times and the duration the entrance and exit doors open, the solar gains, the wind speed and direction, the temperature of the roof, the state of the condenser, and the state of the HVAC units should be measured.

5.1.4 Differentiating between causes

To differentiate between the causes, additional monitoring can be carried out. While specific information concerning analysis and comparison of results will be discussed in Section 6, a general introduction is included here since it requires additional sensors. To preliminarily differentiate between rain and subgrade moisture, the relative humidity in the South wall on the interior and exterior sides can be compared above the rising damp, within the rising damp, and near ground level. Additionally, the correlations between relative humidity in the interior and exterior sections of the wall for 1) soil moisture on the interior and 2) soil moisture on the exterior of the wall can be compared. To tell the difference between rain and interior water vapor, the relative humidity of the interior of the wall and the exterior of the wall can be compared. This should be done above the rising damp line, to exclude any effects from subgrade moisture. To tell the difference between rain and exterior vapor, the relative humidity of the interior and exterior of the wall, during a rain event and not during a rain event can be compared. This should again be done above the rising damp line. To tell the difference between subgrade moisture and interior vapor, the relative humidity on the interior of the wall should be compared above and below the rising damp line. To tell the difference between subgrade moisture and exterior vapor, the relative humidity on the interior and exterior of the wall should be compared during a humid day and not on a humid day above and below the rising damp line. These would be preliminary approaches for differentiating between disparate moisture sources. Additional discussion in Section 6 provides an in depth, quantitative method for elucidating and quantifying the effects of each specific cause on specific parts of the southern wall.

5.1.5 Additional monitorable parameters related to deterioration

In addition to monitoring the parameters previously mentioned, the salinity of the soil inside and outside of the wall can be measured to understand any possible damage mechanisms related to soluble salts. These salts can be identified through microchemical spot-testing so that critical relative humidity cycles can be determine.[49] Besides salinity, acidity can also be a cause of

[49] Odegaard, Nancy, Scott Carroll, and Werner S. Zimmt. 2000. *Material Characterization Tests for Objects of Art and Archaeology.* London: Archetype Publications Ltd.104, 124,108.

deterioration. Thus, it is recommended that the pH of the soil as well as the pH of the rain are monitored.

5.1.5 Proposed locations

The proposed locations for the sensors can be seen in Figures 10 and 11. Sensors which could be placed out of sight from visitors were placed on the roof to both minimize visitors interacting with the equipment and aesthetic effects. Additionally, signage should be placed wherever the sensors are visible to visitors indicating not to touch the equipment.

5.2 Specific sensors for monitoring

Based on the monitorable parameters described above, the following sensors have been chosen for this project. A complete matrix with information about the proposed sensor, catalog number, web address, location, accuracy, resolution, measurement range, and drift can be found in Appendix VII. Information about calibration and installation for all sensors can be found at the links provided in Appendix VII. The project is planned for 1 year of monitoring, which means that the sensors will not need to be replaced based on the manufacturer-listed expected battery life. Concerns about data management and offloading data at appropriate times can be found in Section 5.3.

5.2.1 Relative humidity and temperature within the wall, in the air, and on the roof

On the South wall, this will be measured using a 12-bit Temperature/ Relative Humidity Smart Sensor 6-8" by Onset connected to an RX3000 data logger. This sensor will be placed within the wall at three heights on the South wall interior and exterior (8-11" above the ground, $0.5h_{rising\ damp}$, and $1.1h_{rising\ damp}$) as well as on the interior control wall at a height of $0.5h_{rising\ damp}$ (Figures 10 and 11). Additionally, one sensor will be placed on the southern roof exterior to measure exterior conditions, one will be placed on the southern roof interior to monitor how hot the roof gets, and one will be placed on the interior of the southern wall. Data will be recorded from these sensors every 20 minutes for 1 year; discussion of the data management plan can be found in Section 5.3. This device can be used within temperature ranges of -40°F to 167°F and relative humidity ranges of 0-100%. Based on previous data (see Appendix IV), this sensor is appropriate for this application. Considering the sensor's temperature accuracy of $\pm$ 0.38°F from 32°F to 122°F is 8% of the daily fluctuation in San Antonio temperatures in 2018, the resolution of 0.04°F is 1% of those fluctuations, and the drift over a year of 0.18°F is 5% of those fluctuations, this is an appropriate sensor choice[50]. Again, considering the relative humidity accuracy of 2.5% is 7% of the daily fluctuations in relative humidity in San Antonio, the resolution of 0.1% is 0.2% of those fluctuations, and the drift over a year is 1%, this is acceptable sensor choice[51].

[50] "National Centers for Environmental Information." National Climatic Data Center. Accessed December 16, 2018. https://www.ncdc.noaa.gov/.

[51] "Annual Average Humidity in Texas." Current Results. Accessed December 16, 2018. https://www.currentresults.com/Weather/Texas/humidity-annual.php.

5.2.2 Soil moisture

Soil moisture will be measured using a EC5 Soil Moisture Smart Sensor by Onset connected to a RX3000 data logger 2" below the ground on both the interior and exterior of the southern wall (Figure 10). 2" is recommended because it will isolate only rain water and excludes subgrade moisture sources. Additionally, as it is a clayey soil[52], the soil can hold about 8" worth of water so this placement is well-within the area which would be saturated due to rain water.[53] Notes on the installation on this sensor can be found at the appropriate link in Appendix VII. The use of ground penetrating radar (GPR) to detect subterranean graves or other objects is recommended as to not disturb the integrity of the sight. Methodologies for identifying locations of graves using GPR can be found in the literature.[54] [55] [56] Data will be recorded from the soil moisture sensors every 20 minutes for 1 year; discussion of data management plan can be found in Section 5.3. This device can be used between 0 and 0.550 (m3/m3); as clayey soil on average is 0.2m3/m3, this is an acceptable value.[57] The accuracy in terms of soil moisture is 0.031m3/m3 from 32 to 122◦F. The average soil moisture content from previous testing (at locations B-1 and B-4, see Appendix VIII) is 0.19 ± 0.04 m3/m3. Since this is smaller than the standard deviation and less than 25% of the average value it should not impact the measurement quality.

5.2.3 Rain amount and intensity

Rain amount and intensity will be measured using a HOBO Rain Gauge Data Logger positioned on the roof of the structure (Figure 10). The rain gauge can measure 5 inches of rain per hour. As this rate is higher than the classification even for a "violent" storm (2 in/hour), this is an acceptable limit.[58] The resolution of the rain gauge is 0.01 inches which additionally is acceptable for this application.

5.2.4 Solar radiation

Solar radiation will be measured using a Solar Radiation Smart Sensor by Onset connected to a RX3000 data logger positioned on the roof of the structure (Figure 10). The measurement range is 0 to 1280 W/m2. Considering climate data from previous years (Appendix IV) where the maximum is

---

[52] Raba-Kistner Consultants, INC, *Soil and Groundwater Study Progress Report No. 1 The Alamo Shrine San Antonio, Texas*, technical report (1984).

[53] Alberta Agriculture and Forestry. "Soil Moisture and Temperature Consideration." Alberta Agriculture and Forestry. January 06, 2012. Accessed December 16, 2018. https://www1.agric.gov.ab.ca/$department/deptdocs.nsf/all/crop1272.

[54] Unterberger, R. R. "Ground penetrating radar finds disturbed earth over burials." In *Fourth International Conference on Ground Penetrating Radar*. 1992.

[55] Ruffell, Alastair, Alan McCabe, Colm Donnelly, and Brian Sloan. "Location and assessment of an historic (150–160 years old) mass grave using geographic and ground penetrating radar investigation, NW Ireland." *Journal of forensic sciences* 54, no. 2 (2009): 382-394.

[56] Buck, S. "Searching for graves using geophysical technology: field tests with ground penetrating radar, magnetometry, and electrical resistivity." *Journal of Forensic Science* 48, no. 1 (2003): 1-7.

[57] "Northeast Region Certified Crop Adviser (NRCCA) Study Resources." Certified Crop Advisor Study Resources (Northeast Region). Accessed December 16, 2018. https://nrcca.cals.cornell.edu/soil/CA2/CA0212.1-3.php.

[58] Met Office. "Fact Sheet No. 3 -- Water in the Atmosphere." *National Meteorological Library and Archive*, 2012. Accessed December 16, 2018.

2050 Btu/sqft/day (270 W/m2), this is an acceptable range. Considering that the accuracy is $\pm$ 5%, the resolution is 1.25 W/m2, and the drift is less than $\pm$ 2%, this device's specifications are acceptable for this project.[59] Additionally the spectral range of this sensor (300 to 1100 nm) covers 85% of the solar radiation from the sun and sky which is again an acceptable limit for this project.

5.2.5 Wind speed and direction

Wind speed and direction will be measured using a Wind Speed and Direction Set Smart Sensor by Onset connected to a RX3000 data logger positioned on the roof of the structure (Figure 10). The measurement range is 0 to 170 mph. Considering wind speed data from previous years (Appendix IV) where the maximum monthly average is 14 knots (16 mph), this is an acceptable range. Considering that the accuracy of $\pm$ 2.4mph is 17% of the average and the resolution of 1.1mph is 8% of the average, this sensor is acceptable for this application.

5.2.6 Groundwater level

Groundwater levels will be measured using a HOBO Bluetooth Low Energy Water Level Data Logger with 30' range positioned on the exterior of the south wall as seen in Figure 10. As the groundwater level is approximately at 17' in the position of interest (see Appendix VIII), this is an acceptable range. Considering that the accuracy of $\pm$0.015 ft is 4% of the average daily fluctuation in San Antonio groundwater levels in 2018 and the resolution is 2% of those fluctuations, this is acceptable.[60]

5.2.7 Duration and number of times doors are open

The state of the entrance and exit doors will be measured using a HOBO Extended Memory State Data Logger positioned on both the entrance and exit doors (Figures 10 and 11). The resolution of 1 event is acceptable for this application since it is a small fraction of the expected visitation. As this sensor can only accept 346,795 total measurements, only the periods starting in January running until the door has been opened 346,795 times and similarly starting again in July and running for 346,795 state changes will be monitored (Figure 12). Data for ticket sales was approximated knowing the peak visitations months and expected visitation totals (2 million). Plans for data management and trips to off load data are discussed below in data management. During the final data processing stages, a plot of the door state versus the number of tickets sold can be created. A line of best fit can be placed through the data and used to extrapolate unmonitored door states.

[59] Campbell Scientific. "Solar Radiation." Campbell Scientific. Accessed December 16, 2018. https://s.campbellsci.com/documents/us/category-brochures/b_solar-radiation.pdf.

[60] "Official Aquifer Level & Statistics." San Antonio Water System. Accessed December 16, 2018. https://www.saws.org/Your_Water/aquifer/.

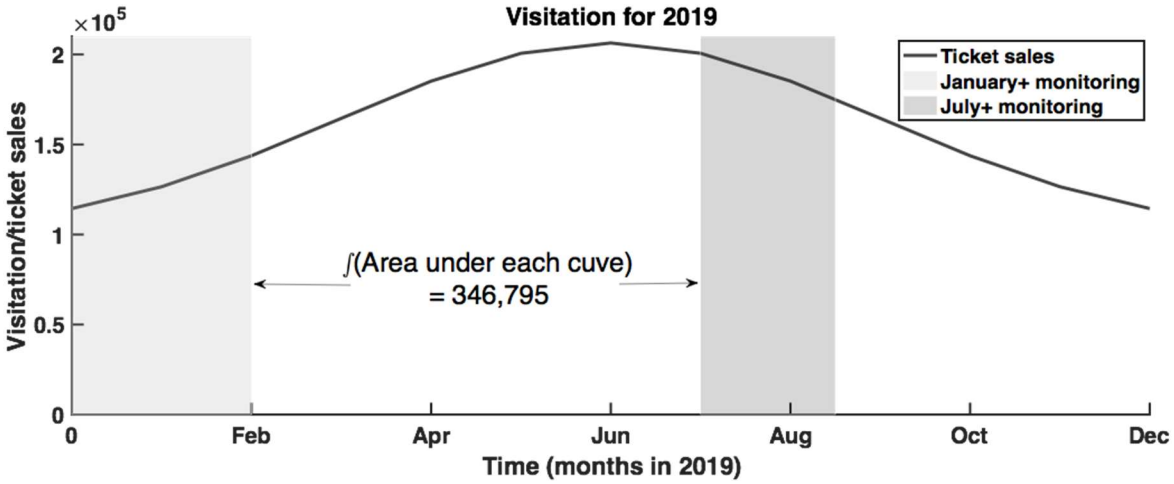

Figure 12: Plot of projected visitation over time in 2019 with an overlay of the monitoring periods for the state of the entrance and exit doors.

5.2.8 Condenser and ac on/off state

The state of the condenser and ac units will be measured using a HOBO Extended Memory Motor On/Off Data Logger positioned on the AC units and specifically on the condenser that has failed previously (Figures 10 and 11). The resolution of 1 event is acceptable for this application.

5.2.9 Salinity of the soil

The salinity of the soil will be measured using a HOBO Salt Water Conductivity/ Salinity Data Logger connected to a RX3000 data logger positioned in the soil on the interior and exterior of the building (Figure 10). Considering that the typical salinity of soil in Texas is 0.5-2.5 dS/m and the range of this sensor is 0.1-10 dS/m, this is an acceptable instrument. Additionally, considering that the accuracy of the conductivity is 2uS/cm which is 2% of the average value, this is an acceptable instrument[61].

5.2.10 Ph of Soil and Rain

The Ph of the soil and the rain will be measured using the HOBO Bluetooth Low Energy pH and Temperature Data Logger positioned in the soil and on the roof as shown in Figure 10. Given that the average soil pH in San Antonio is 8.2[62], the average pH of the rain in San Antonio is 7.7-8[63], and the range of the instrument is 2-12pH, this instrument is appropriate.

[61] Miyamoto, S. "Supplement to Diagnosis and Management of Salinity Problems in Irrigated Pecan Production: Salt Leaching." *Texas Water Resources Institute Technical Report No. 387A*, 2010. Accessed December 16, 2018.

[62] Harris, Tom. "Living with Caliche." My San Antonio. October 26, 2005. Accessed December 16, 2018. https://blog.mysanantonio.com/waytogrow/2005/10/tom-harris-living-with-caliche/.

[63] Lucero, Sarah. "Verify: Is Alkaline Water Healthier than Regular Tap Water?" KENS5. June 15, 2017. Accessed December 16, 2018. https://www.kens5.com/article/news/local/verify/verify-is-alkaline-water-healthier-than-regular-tap-water/449171086.

5.3 Discussion about data loggers and data retrieval timeline

In the cases where the sensor is not already connected to its own data logger, the RX3000 has been selected as the data logger. This data logger has 15 channels and can store 43,300 measurements. Accounting for the different channels required by the sensors, the layout of the necessary data loggers can be found in Figures 10 and 11. As there is 100% cellular coverage in San Antonio, the US Max-Connect Cellular Plan is recommended for the RX3000 Data Plan[64]. Figure 13 provides a breakdown of when data needs to be transferred off the sensors; calculations for this can be found in Appendix IX. The RX3000 can send an email once a month with all the data. At this point the data will be backed up on several external devices and wiped from the logger to ensure there is enough capacity for the next month's measurements. The intervals for data retrieval of the other devices which have their own loggers can also be seen in Figure 13. Similarly, calculations for necessary intervals can be found in Appendix IX.

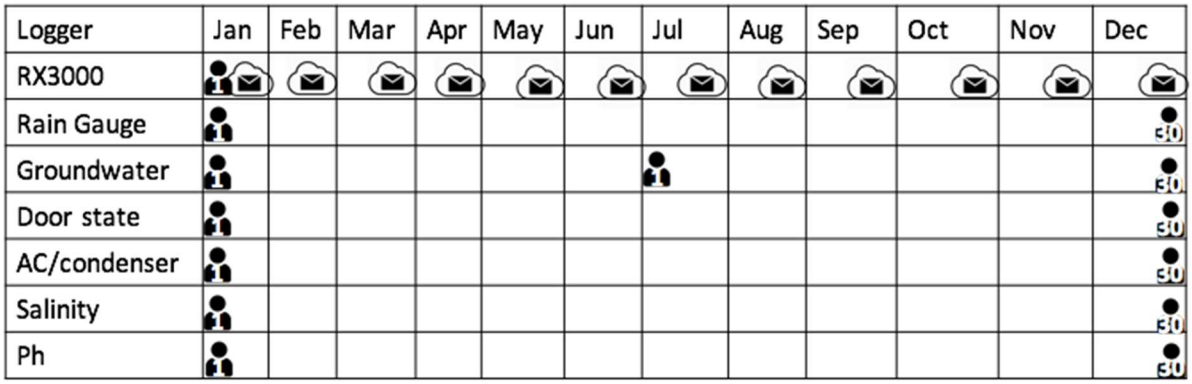

Figure 13: Icons indicate a person on site, letter in cloud is automatic data delivery to email. All automatic emails will happen on the 30th of the month. As the dates the person would go varies, it has been included as the number on the icon.

5.4 Discussion about data processing

HOBOLink will be used throughout the monitoring period to ensure that sensors are working as anticipated and to see any preliminary correlations in data sets. Additional sensors and testing can be utilized if needed based on these preliminary results. For more detailed data processing, the data will be loaded into MATLAB. Procedures for retrieving the data from each sensor can be found in Table 1. Additional information about data processing in MATLAB can be found in Section 6.

[64] Holmes, Chris. "Best Cell Phone Carriers and Coverage in San Antonio." WhistleOut. November 13, 2018. Accessed December 16, 2018. https://www.whistleout.com/CellPhones/Guides/Best-Plans-in-San-Antonio.

Table 1: List of data retrieval methods and links for data transfer instructions

Method of data retrieval	Associated sensors	Link for data transfer instructions
HOBOLink	Any sensors using a RX3000 data logger	https://www.onsetcomp.com/products/software/hobolink
HOBO optic USB base station	HOBO Rain Gauge Data Logger, HOBO Salt Water Conductivity/ Salinity Data Logger	https://www.onsetcomp.com/files/manual_pdfs/10655-G-MAN-BASE-U-4.pdf
Direct read cable	HOBO Bluetooth Low Energy Water Level Data Logger	https://www.onsetcomp.com/files/manual_pdfs/19389-J%20MX2001%20Manual.pdf
USB	HOBO Extended Memory Motor On/Off Data Logger, HOBO Extended Memory Motor On/Off Data Logger	Traditional USB transfer methods can be used here
Bluetooth HOBO Mobile App on iOS or Android	HOBO Bluetooth Low Energy pH and Temperature Data Logger, HOBO Bluetooth Low Energy pH and Temperature Data Logger	https://www.onsetcomp.com/hobomobile/

6. PROPOSED METHOD FOR ANALYSIS AND INTERPRETATION OF DATA

The aim of this work is to quantify and evaluate how the following systems are related to the moisture content of the wall:

a. Cycling of interior and/or exterior relative humidity
b. Rain (near surface soil moisture)
c. Subgrade moisture (lower aquifer)

Salinity and other damage mechanisms are assumed to be related to moisture content which can be measured via relative humidity. There are five main stages to the analysis (Figure 14): I) checking overall relationships between the southern wall and the control wall located on the interior of the building, II) checking the influence of cycling interior and/or exterior relative humidity, III) checking the influence of rain and near surface moisture, IV) checking the influence of subgrade moisture, and V) quantifying the relative influence of the three sources on the moisture content of the wall.

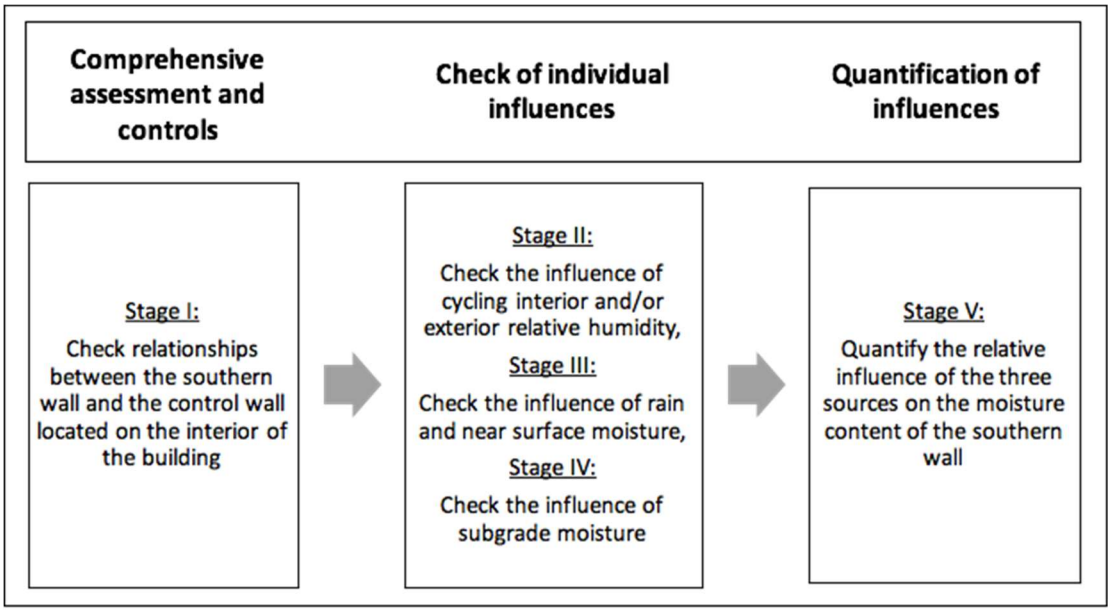

Figure 14: Stages of data analysis and suggested order

6.1 Checking overall relationships (Stage I)

First, the overall relationships between the relative humidity sensors in the southern wall and the interior wall should be checked to ensure that the sensors are working as expected and to get a preliminary assessment of how interior and exterior factors are related to the relative humidity of the wall. To do this, the relative humidity at both locations (interior and exterior) and at all three heights should be plotted against time for the following periods: annual, the month with highest precipitation, the month with highest exterior relative humidity, the month with lowest precipitation and lowest exterior relative humidity, and the month with the highest visitation (Figure 15). On the right of Figure 15, the six relative humidity sensors can be seen with their identifying labels. The label indicates that they are on the south wall (S), then the position (I for interior, E for

exterior), then the height (1 for at the base, 2 for in the middle of the rising damp, and 3 for above the rising damp).

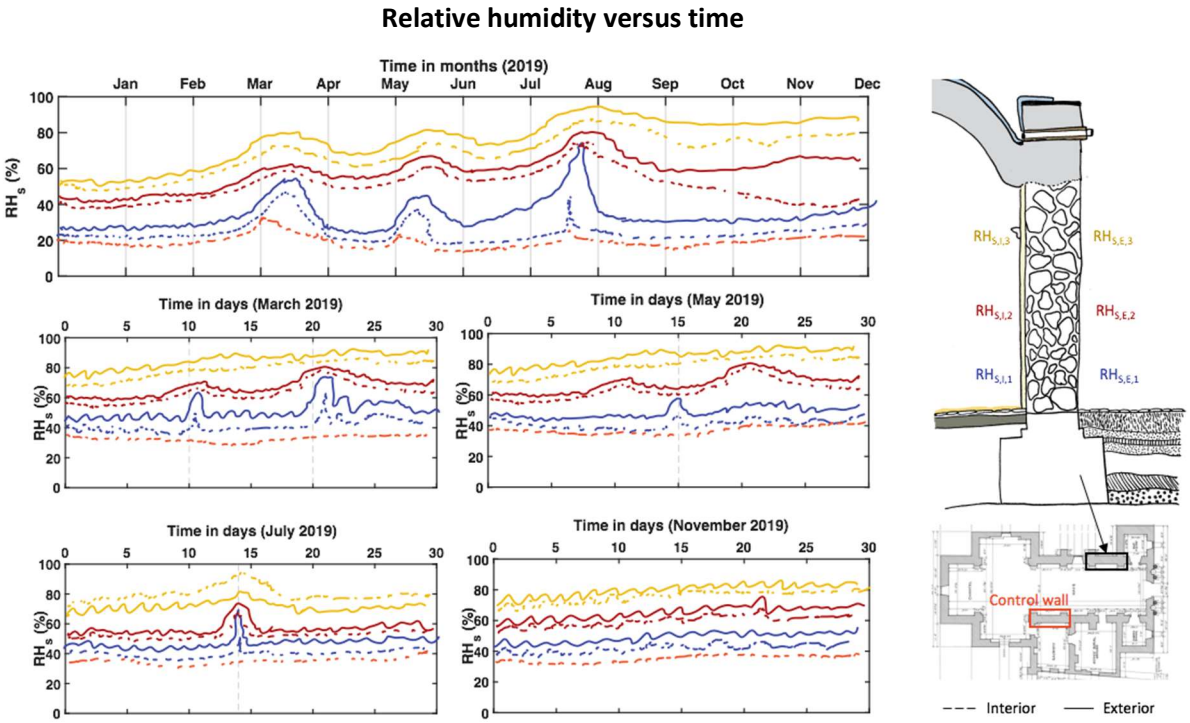

Figure 15 : Plots of relative humidity measured inside the walls for different increments of time. Both the south wall and the control wall are plotted. Grey lines in the annual figure separate months to aid in reading the graph, the dashed grey lines for the March plot correspond to rain events, the dashed grey lines in the May plot correspond to a peak in exterior relative humidity, and the dashed grey lines in the July plot correspond to a peak in visitation.

While the annual time period might be able to provide overall correlations, the data itself will be very noisy. Thus, by considering only select months, any patterns emerging will be more clear. Additionally, vertical lines will be graphed on the individual month plots to indicate key events. As this monitoring has not yet been carried out, placeholder months have been assigned for the purposes of discussion and by no means represent real data or projects of real data. Events such as days it rained (in March for example), the day with the highest humidity (May), and the day with highest visitation (July) could be included. Considering Figure 15, the following questions (Figure 16) can be asked and relevant next steps can be addressed.

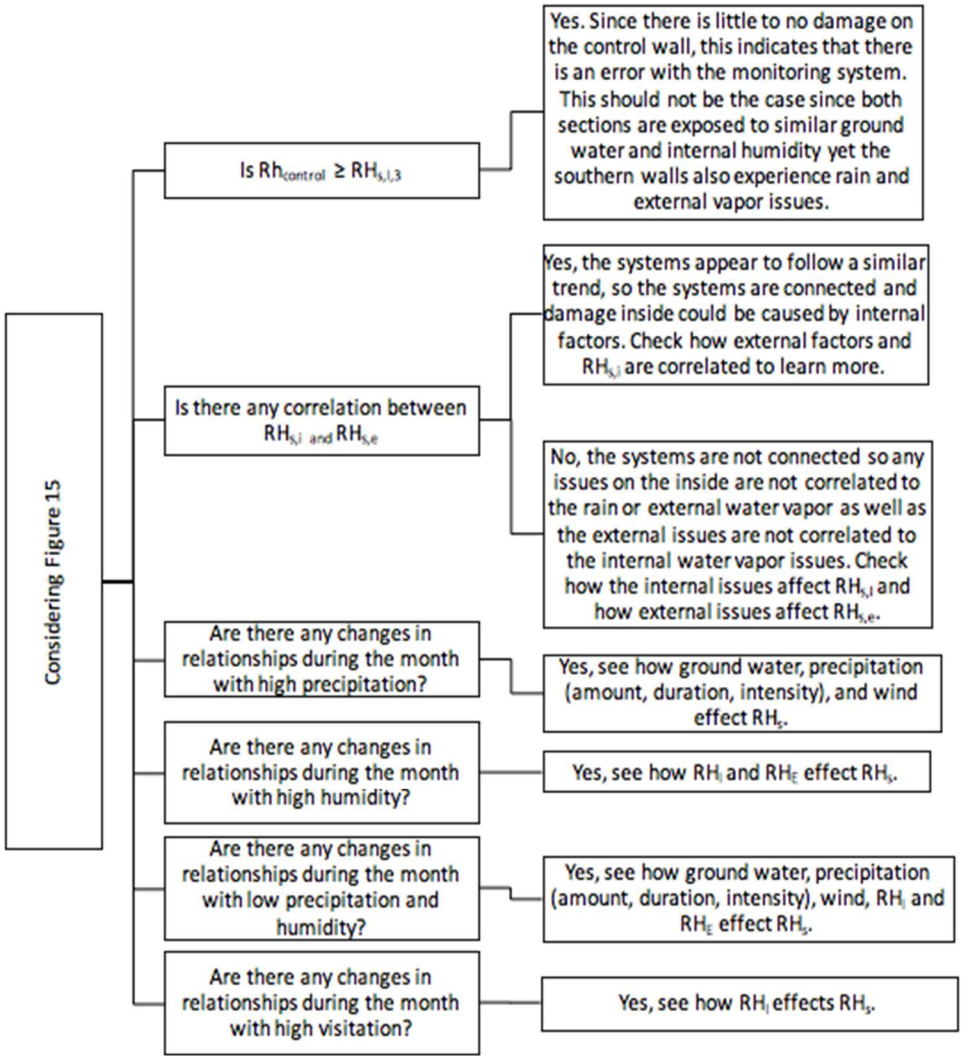

Figure 16: Example of a non-exhaustive decision diagram for understanding Stage I data analysis.

6. 2. Checking the influence of cycling interior and/or exterior relative humidity (Stage II)

To gain an initial understanding of the influences of relative humidity cycling the following monitored and collected parameters should be plotted against a year of time (Figure 17): exterior air temperature ($T_{air,E}$), the condenser state, interior air temperature ($T_{air,I}$), combined air conditioning loads (AC_{total}), relative humidity of the interior air ($RH_{air,I}$), relative humidity of the south wall at all three positions for interior and exterior ($RH_{S,x,y}$ where S indicates on the south wall, x indicates interior or exterior, and y indicates the height), relative humidity of the exterior air ($RH_{air,E}$), the opening of doors, solar gains, and speed of winds directed at the south wall.

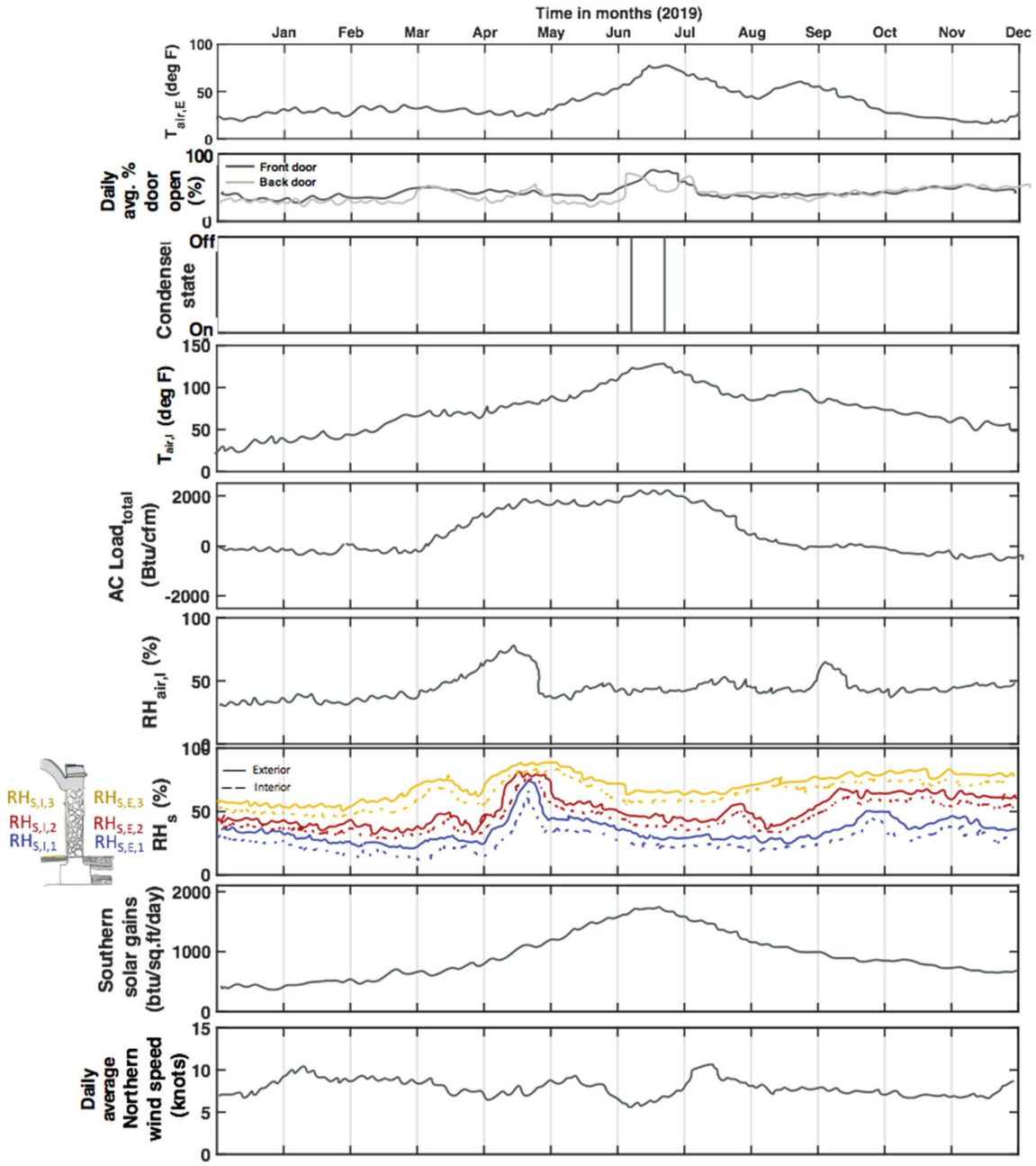

Figure 17: Plots of parameters relevant to relative humidity cycling over the course of a year

If there are periods within the span of a year which yield interesting patterns, the data can be examined for subsets of time. For example, if there is a month where there is exceptionally high relative humidity in the wall, the parameters could be examined for that month only (Figure 18).

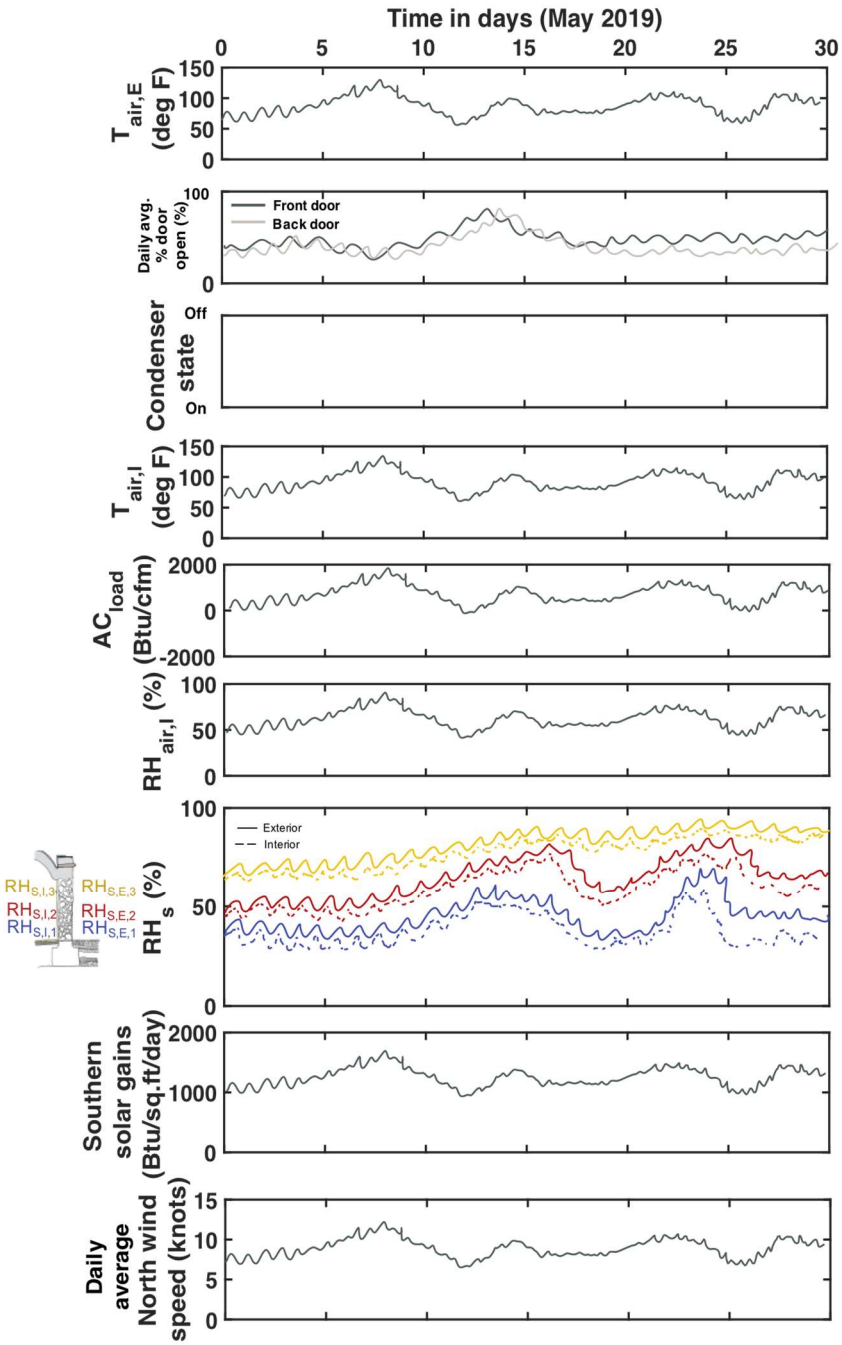

Figure 18: Plots of parameters relevant to relative humidity cycling over the course of a month

If there is a preliminary relationship between the cycling of interior and/or exterior relative humidity and a certain parameter, then this parameter of interest should be compared to $R_{S,x,y}$ using a cross-correlation plot to quantify any existing correlation. X and y will vary based on the parameter of interest. The number of samples can be exhaustive or subsampled to include a specific period of interest. Cross-correlation plots are more robust than just the use of the coefficient of determination (R^2) as cross-correlation plots account for not only the average correlation of the

data but also the standard deviation of the data's correlation. Figure 19 is an example series of potential cross-correlation plots. For this example, the relationship between $RH_{air,E}$ and the relative humidity on the interior and exterior of the south wall has been examined for all sensor heights as it could be a potential parameter of interest based on discussion of moisture sources in Section 4.

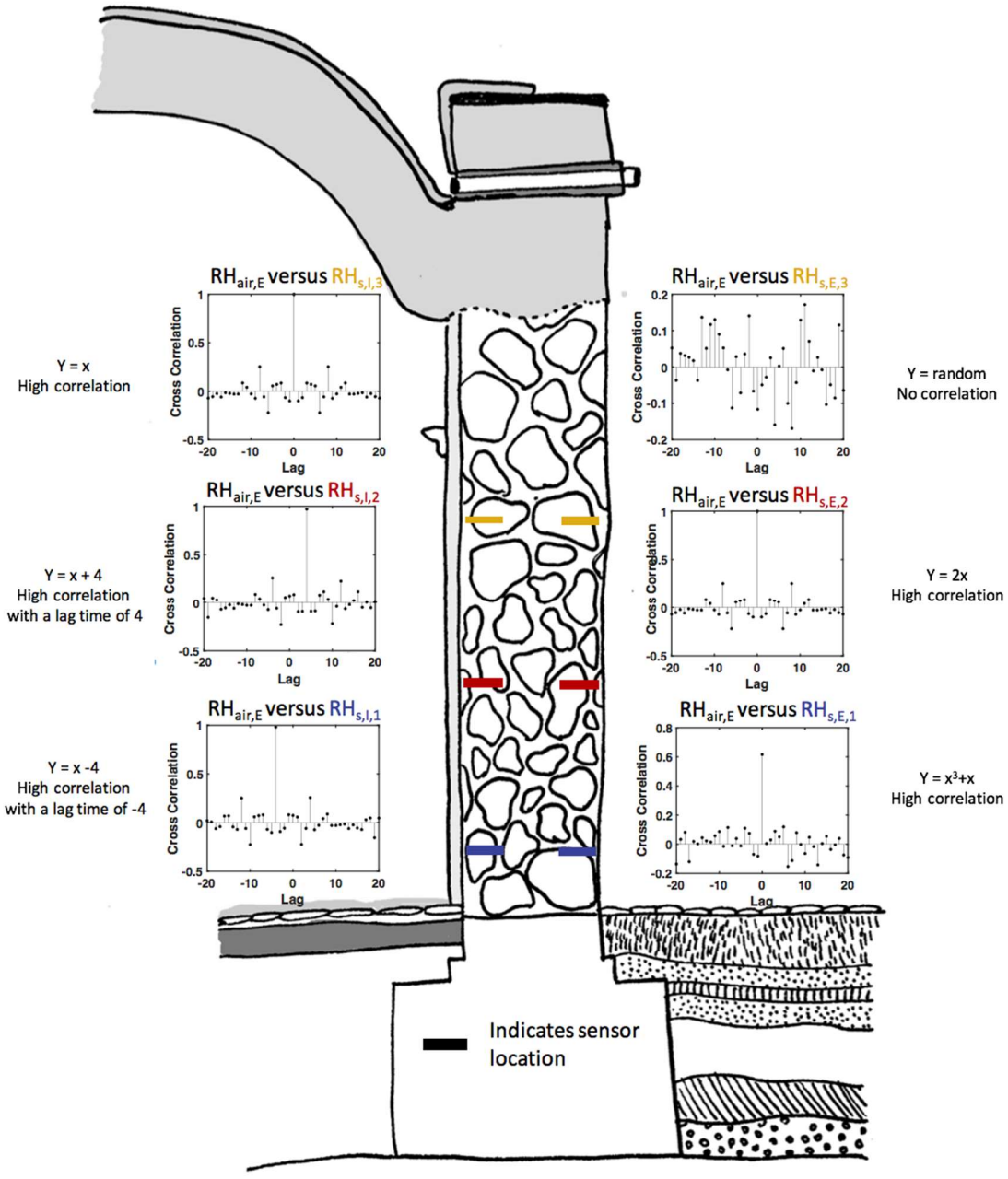

Figure 19: Examples of cross-correlation plots where x was a set of random numbers and the equations for y are shown. This method was shown to work for linear and non-linear relationships.

To ascertain how correlated the sets of data are and any possible lag between the datasets, the MATLAB procedure outlined in Figure 20 can be followed.

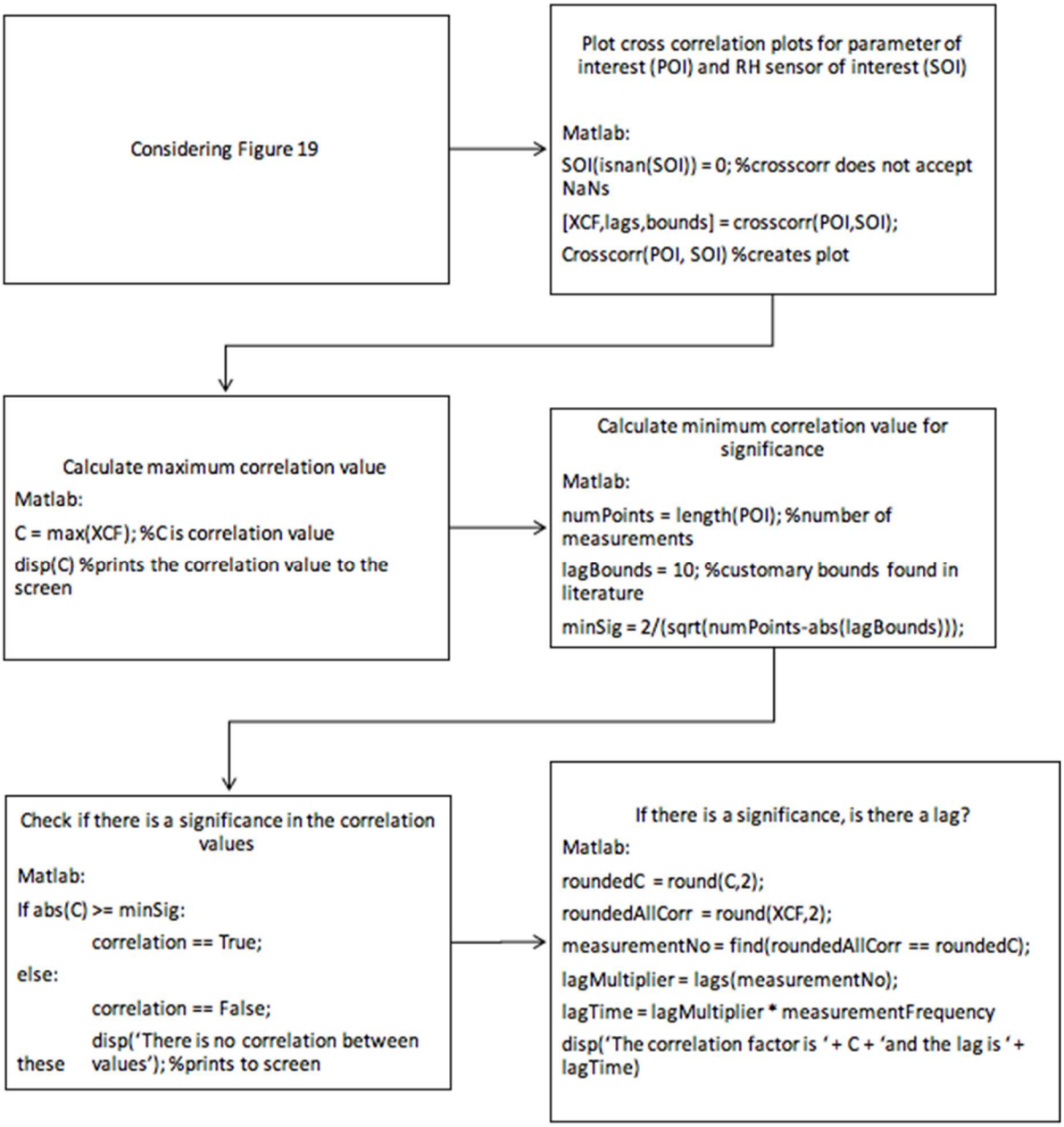

Figure 20: Method for distilling cross-correlation plots down to a single number in MATLAB

Once the correlation (C) between the parameters of interest and the $RH_{S,x,y}$ are calculated, a matrix can be created such as the one in Table 2. It can be colored to indicate varying levels of correlation; Table 2 it is colored from red to green where red represents no correlation and green represents high correlation. Using this color-coded matrix, the correlation between disparate parameters of

interest and the relative humidity in the wall can be quantified, compared, and assessed. A potential line of inquiry for these types of results, can be seen in Figure 21.

Table 2: Sample results from distilling the results of cross-correlation plots. Colors are used for fast comparison of parameters.

Location →	I1		I2		I3		E1		E2		E3	
Parameter ↓	C	lag	C	lag	C	lag	C	lag	C	lag	C	lag
$T_{air,i}$	0.99	1	0.99	1	0.98	1	0	N/A	0	N/A	0	N/A
$RH_{air,e}$	0	N/A	0	N/A	0	N/A	0.91	2	0.92	2	0.87	2
AC_t	0.97	3	0.96	3	0.97	5	0	N/A	0	N/A	0	N/A

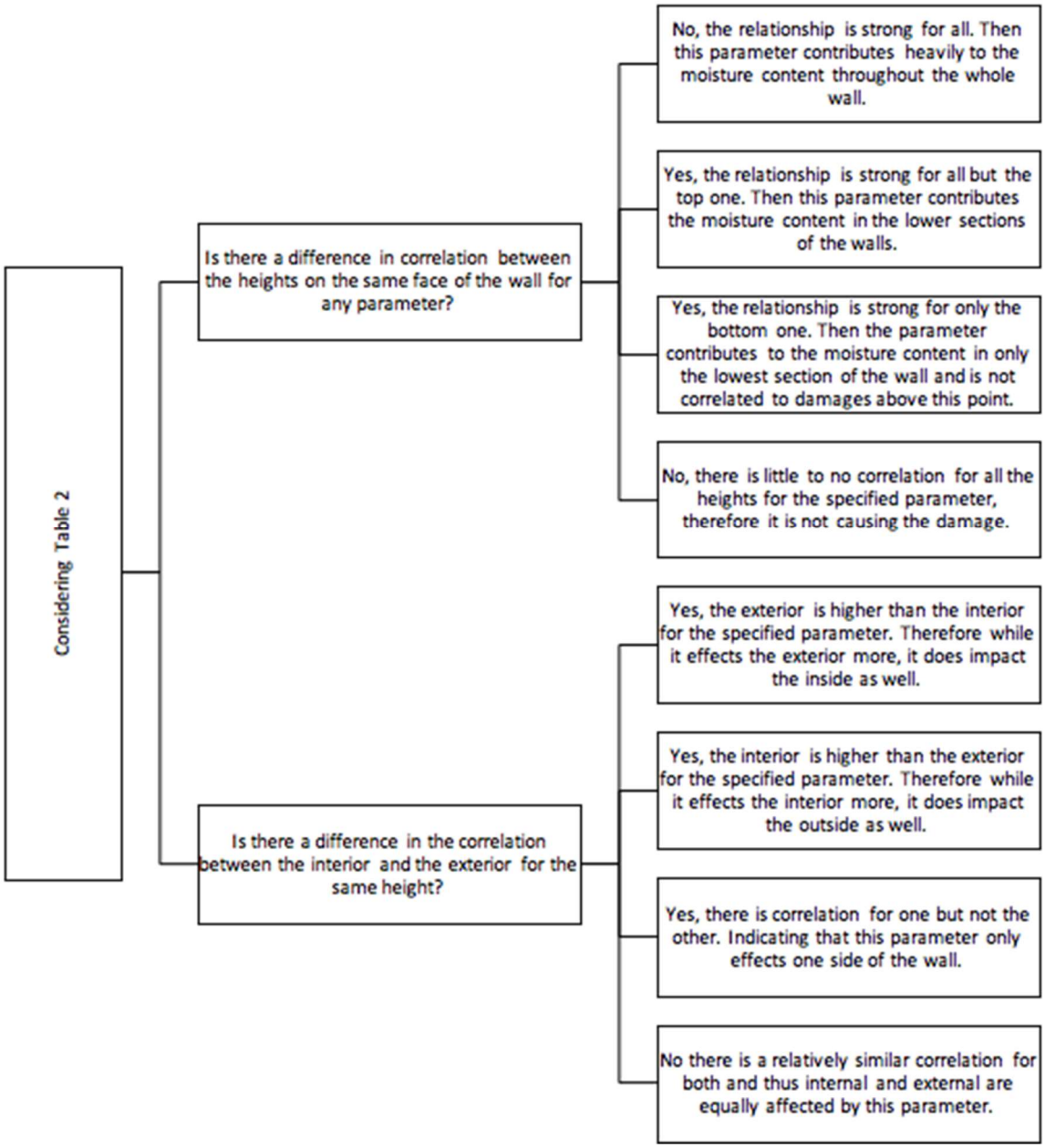

Figure 21: Example of a non-exhaustive line of inquiry when examining the results of Figure 20.

6.3 Checking the influence of rain and near surface soil moisture (Stage III)

Similar to the approach in Stage II, to gain an initial understanding of the influences of rain and near surface soil moisture, the following monitored and collected parameters should be plotted against time: soil moisture (c), rain amount (R_{amt}), rain intensity (R_{int}), rain duration (R_{dur}), relative humidity of the south wall at all three positions for interior and exterior ($RH_{S,x,y}$) (Figure 22).

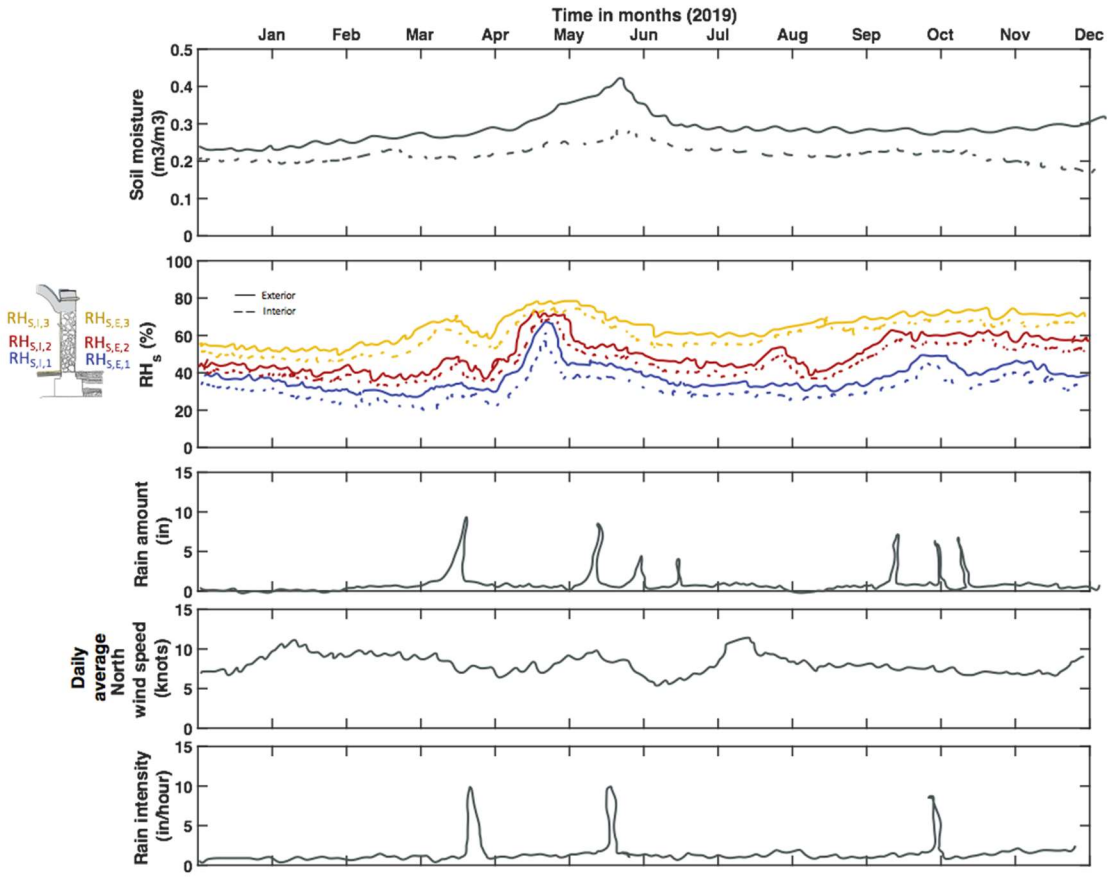

Figure 22: Plots of parameters relevant to rain and near surface moisture over the course of a year

Similar to above, data from specific months can be subsampled and plotted as well as if there is a preliminary relationship between the influence of rain and near surface soil moisture and a certain parameter, then this parameter of interest should be compared to $RH_{S,x,y}$ using a cross-correlation plot. Again, once the correlation (C) between the parameters of interest and the $RH_{S,x,y}$ are calculated, a matrix can be created and colored to indicate varying levels of correlation. Using a color-coded matrix, the correlation between disparate parameters of interest and the relative humidity in the wall can be quantified, compared, and assessed. A similar line of inquiry to that outlined in Figure 21 can be followed.

6.4 Checking the influence of subgrade moisture (Stage IV)

Similar to the approaches in Stages II and III, to gain an initial understanding of the influences of influence of subgrade moisture, groundwater level (GW) and relative humidity of the south wall at all three positions for interior and exterior ($RH_{S,x,y}$) should be plotted against time (Figure 23).

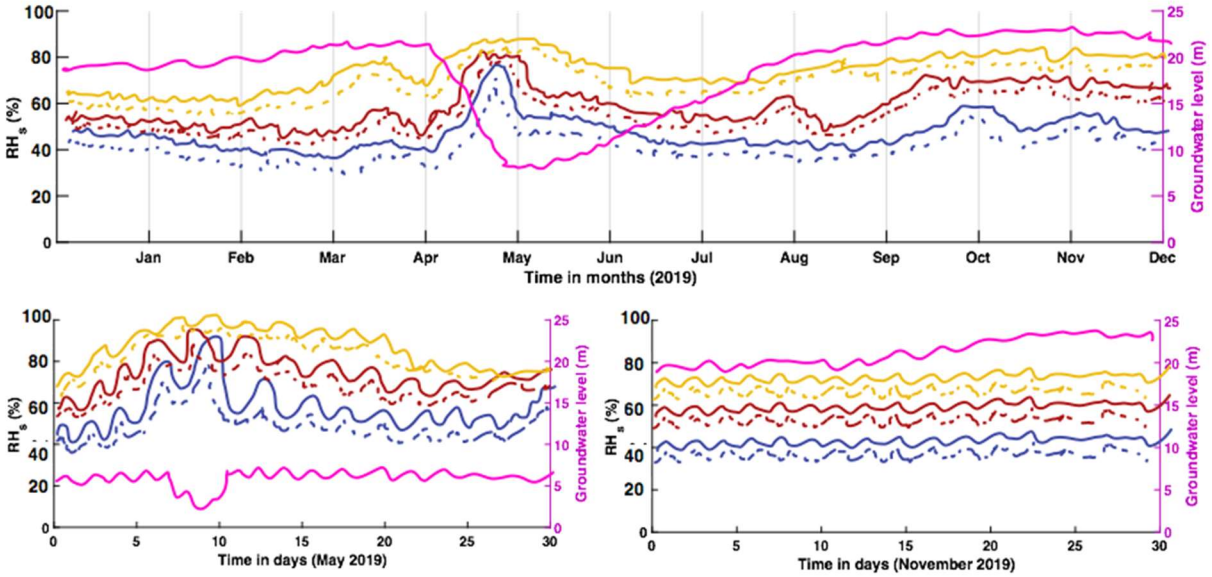

Figure 23: Plots of parameters relevant to groundwater levels over the course of a year and for specific months of interest.

Similar to above, data from specific months can be subsampled and plotted as well as if there is a preliminary relationship between the influence of subgrade moisture and the relative humidity of the wall, then the groundwater levels should be compared to $RH_{S,x,y}$ using a cross-correlation plot. Again, once the correlation (C) between the parameters of interest and the $RH_{S,x,y}$ are calculated, a matrix can be created and colored to indicate varying levels of correlation. Using a color-coded matrix, the correlation between groundwater level and the relative humidity in the wall can be quantified, compared, and assessed. A similar line of inquiry to that outlined in Figure 21 can be followed.

6.5 Quantifying the influence of the three sources on the moisture content of the wall (Stage V)

While it is important to understand how the different sources of moisture are related to the relative humidity of the wall, actionable information is a desired outcome of this proposal. Therefore, the relative influence of the three sources of water on the moisture content of the wall should be quantified and compared to each other to facilitate an informed hierarchy of damage mechanisms. Based on Figure 9, a series of equations (Eq (1) - Eq (6)) can be generated to understand what percentage of the moisture content in the wall is due to each source at each monitored location. Previously, in Figure 9, the locations were called 'I1', 'E2', etc. Now that the monitoring plan has been established, only sensor names will be used; for instance 'E2' is called $RH_{S,E,2}$where the 'S' stands for the south wall, the E stands for on the exterior, and the 2 stands for position 2 as defined in Figures 9 and 10. The terms on the left side of the equations indicate relative humidity values that can be directly measured with a sensor. The terms on the right side of the equations represent the percent contribution that this source makes to the overall relative humidity measured at this sensor; they do not represent the raw monitoring data for each variable. For instance, GW_1 represents the

amount of relative humidity measured in a particular sensor due to groundwater, not the groundwater levels themselves.

$$RH_{S,I,1} = RH_I + GW_1 \quad \text{Eq(1)}$$
$$RH_{S,I,2} = RH_I + GW_2 \quad \text{Eq (2}$$
$$RH_{S,I,3} = RH_I \quad \text{Eq(3)}$$
$$RH_{S,E,1} = GW_1 + \text{Rain} + RH_E + \text{AW} \quad \text{Eq(4)}$$
$$RH_{S,E,2} = GW_2 + \text{Rain} + RH_E \quad \text{Eq(5)}$$
$$RH_{S,E,3} = \text{Rain} + RH_E \quad \text{Eq(6)}$$

Since the contributions of $RH_I$to the overall relative humidity of the south wall are isolated in I3, the contributions due to groundwater (GW_1 and GW_2) can be found looking at data from sensors $RH_{S,I,1}$ and $RH_{S,I,2}$ during times when the groundwater level is below the level of influence on the southern wall. To calculate the periods of time when the groundwater level is below the level of influence, the time (lag) between when the groundwater level is below the interior soil moisture sensor and when that soil moisture sensor reads as dry is needed. This can be found using the same procedures above for cross-correlation plots. Once the lag time is known, periods of time where the groundwater is below the soil moisture sensor plus the lag time can be subsampled from the dataset. Now if $RH_{S,I,2}$ and $RH_{S,I,1}$ are examined, the effects of groundwater have been removed and only the term for RH_I remains. If it is desired, any non-constant effects of RH_I on the interior of the wall at the different heights can be calculated at this point; for the purposes of simplification, any changes in relative humidity over the course of the wall's height have been approximated as linear. This would yield Equations 7 and 8 where ($\rightarrow 0$) indicates that the term goes to zero.

$$RH_{S,I,1} = \alpha RH_I + GW_1 \ (\rightarrow 0) \quad \text{Eq(7)}$$
$$RH_{S,I,2} = \beta RH_I + GW_2 \ (\rightarrow 0) \quad \text{Eq(8)}$$

If the values of $RH_{S,I,1}$ (now αRH_I) and $RH_{S,I,2}$ (now βRH_I) are plotted against the values of $RH_{S,I,3}(RH_I)$ (Figure 24), the slopes of those lines will be α and β respectively.

Relative humidity sensor measurements at $RH_{S,I,1}$ and $RH_{S,I,2}$ versus $RH_{S,I,3}$ (no rain)

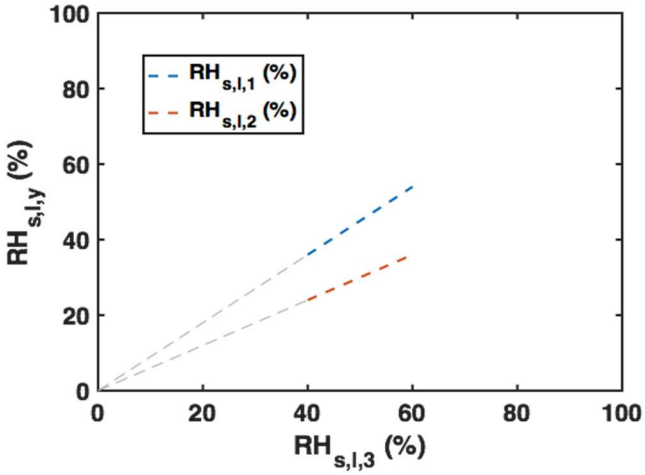

Figure 24: Relative humidity sensor measurements at$RH_{S,I,1}$ and $RH_{S,I,2}$ versus $RH_{S,I,3}$ sampled for time periods with no rain. The slopes of these lines are the constant multipliers for RH_I.

Then if the subsampling is removed and all the values of $RH_{S,I,1}$ ($\alpha RH_I + GW_1$) and $RH_{S,I,2}$ ($\beta RH_I + GW_2$) are plotted against the values of $RH_{S,I,3}$ (RH_I), the y-intercepts of each line will be the contribution of groundwater at that height (Figure 25).

Relative humidity sensor measurements at $RH_{S,I,1}$ and $RH_{S,I,1}$ versus $RH_{S,I,3}$

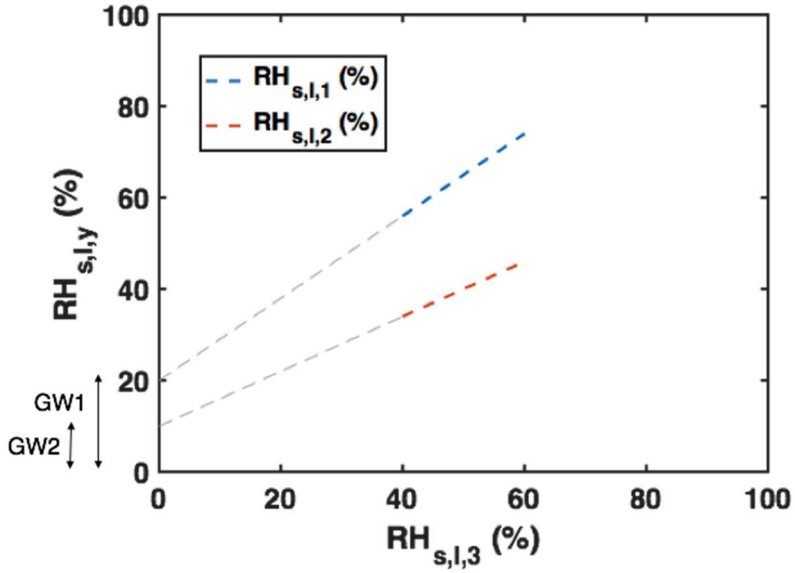

Figure 25: Relative humidity sensor measurements at $RH_{S,I,1}$ and $RH_{S,I,2}$ versus $RH_{S,I,3}$. The y-intercepts of these lines are the influences of groundwater to these particular sensors.

Next RH_E can be isolated if $RH_{S,I,3}$ (RH_E + Rain) is examined during time periods where there is no rain and any effects of rain are accounted for using the longest lag time of the relevant parameters (see lag Figure 26).

Cross-correlation plots of $RH_{S,I,3}$ and Rain measurements

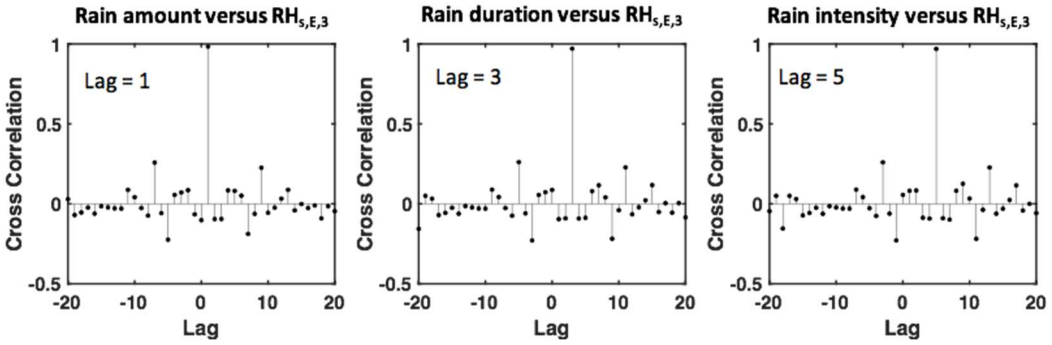

Figure 26: Cross-correlation plots of $RH_{S,I,3}$ and rain amount, rain duration, and rain intensity. Based on these plots, rain intensity would have the longest lag time.

The same non-constant relationships of exterior relative humidity along the height of the wall can be sought using:

$$RH_{S,E,1} = GW_1\ (\rightarrow 0) + \text{Rain}\ (\rightarrow 0) + \gamma RH_E + \text{AW}\ (\rightarrow 0) \qquad \text{Eq(9)}$$

$$RH_{S,E,2} = GW_2\ (\rightarrow 0) + \text{Rain}\ (\rightarrow 0) + \varepsilon RH_E \qquad \text{Eq(10)}$$

If the values of $RH_{S,E,1}$ (now γRH_E) and $RH_{S,E,2}$(now εRH_E) are plotted against the values of $RH_{S,E,3}$(nowRH_E)(figure 27), the slopes of those lines will be γ and ε respectively.

Relative humidity sensor measurements at $RH_{S,E,1}$ and $RH_{S,E,2}$ versus $RH_{S,E,3}$ (no rain)

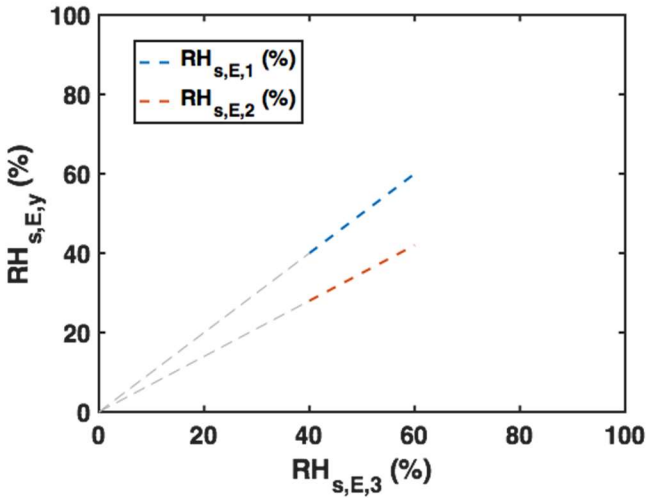

Figure 27: Relative humidity sensor measurements at $RH_{S,E,1}$ and $RH_{S,E,2}$ versus $RH_{S,E,3}$ during periods where there is no rain. The slopes of these lines are the constant multipliers for RH_E.

Then if the subsampling is removed and the effects of GW_2 at each measurement point on the inside are subtracted from $RH_{S,E,2}$ (now εRH_E + Rain), and this result is plotted against $RH_{S,E,3}$ (RH_E+ Rain), the y-intercept will be the effects of rain (Figure 28).

Relative humidity sensor measurements at $RH_{S,E,2}$ versus $RH_{S,E,3}$ (excluding GW_2)

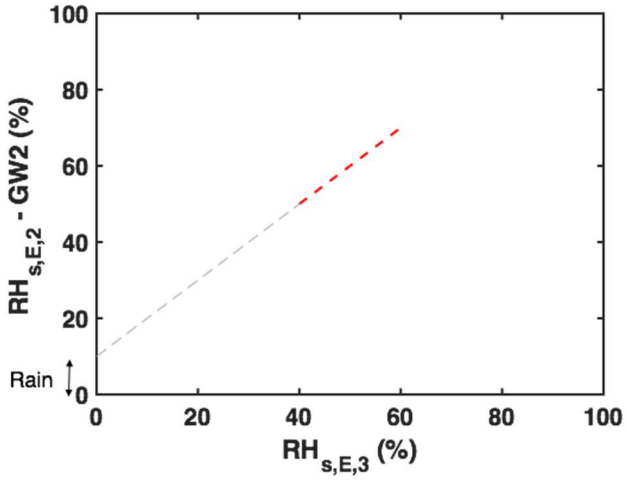

Figure 28: Relative humidity sensor measurements at $RH_{S,E,2}$ (minus the effects of groundwater as calculated for the interior of the wall) versus $RH_{S,E,3}$. The y-intercept is the influence of rain.

If this is done for $RH_{S,E,1}$ (γRH_E + AW+ GW_1 + Rain) where the effects of GW_1 and the effects of rain are subtracted from $RH_{S,E,1}$ (now γRH_E + AW), and this result is plotted against $RH_{S,E,3}$

(RH_E + Rain) minus the effects of Rain (now RH_E), the y-intercept will be the effects of accumulated rain water (AW) near the wall (Figure 29).

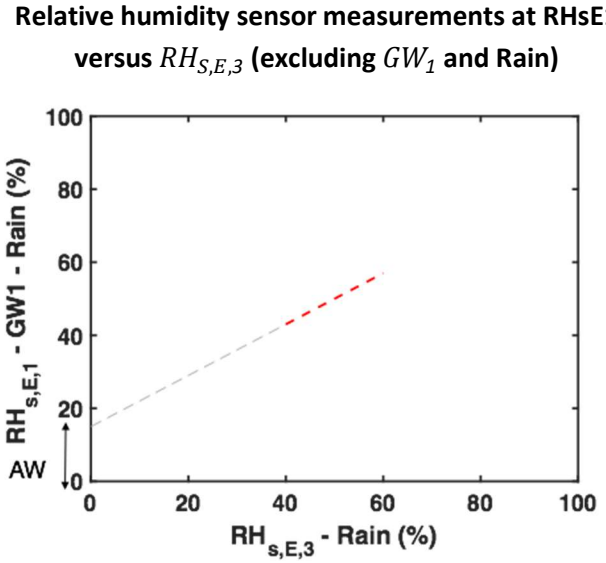

Figure 29: Relative humidity sensor measurements at $RH_{S,E,1}$ (minus the effects of groundwater and rain) versus $RH_{S,E,3}$. The y-intercept is the influence of accumulated ground water.

Once the contributions from the disparate moisture sources are isolated, the average contribution and standard deviation of that contribution for each parameter can be calculated. Using those values, plots (Figure 30) showing how much each parameter influences the relative humidity in a specific region of the wall can be defined. By quantifying the influence of the sources of moisture on the moisture content of the wall, a conservator will be able to create an informed hierarchy of damage mechanisms which could be addressed in future interventions.

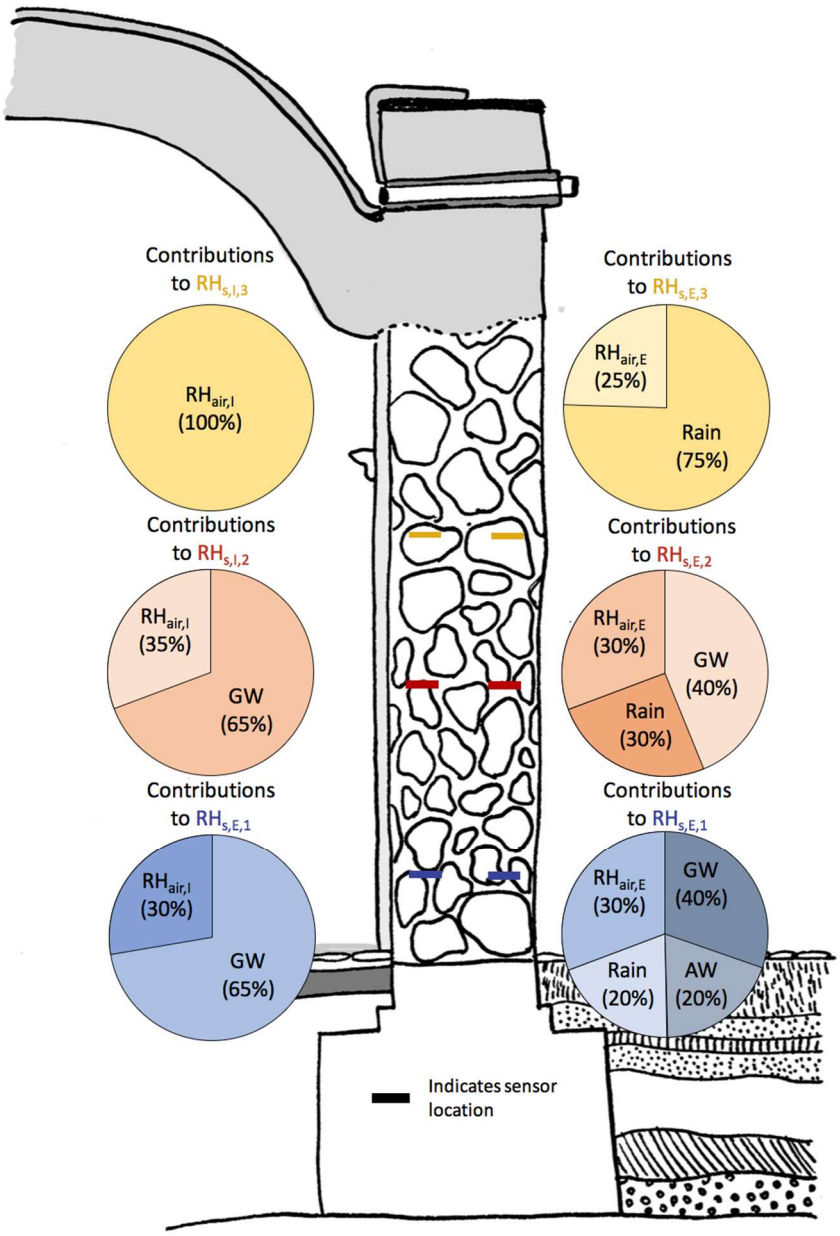

Figure 30: Percentage that each source of moisture contributes to each part of the wall.

6. 6 Correlating water with salinity and pH

Aside from moisture flows into the building, the damage to the structure could be aided by high salt concentrations as well as acidic rain. To understand if these mechanisms are contributing or not, pH and salinity sensors were placed in proximity to the wall (Figure 10). Using these sensors, a preliminary understanding of the concentrations of soluble salts and the strength of acidic rain can be ascertained. In the future, additional on-site testing could be done to examine the salinity within the wall itself at different heights. Additionally, it might be interesting to create cross-correlation plots of the salinity in the wall at different heights versus the different

water intake mechanisms to understand if one of these is more correlated to higher concentrations of soluble salts in the wall. However, this is outside the scope of the present work.

6.7 Summary

Our proposal suggests using nondestructive testing in conjunction with in-situ monitoring to ascertain the predominant drivers of deterioration in La Vieja Misión. As water-related problems are the most prevalent causes of damage in historic buildings, we generated a series of three moisture related working hypotheses. This was done by integrating detailed systems diagrams of the moisture and deterioration sources with information about the site's historical background, previous structural changes, and prior climate data.

The multiple working hypotheses are that the water-related problems could be due to cycling of the interior and/or exterior relative humidity, rain (including near surface soil moisture), and subgrade moisture sources. Subsequent to developing the hypotheses, the systems diagrams and prior climate data were used to optimize the types of sensors which should be instrumented on the wall and the modes of data analysis which are recommended.

With this proposed diagnostic and monitoring plan, we aim to isolate the sources of moisture to different regions on the south wall to understand which predominant mode of moisture flow is the most detrimental to the structure. Quantitative evidence for the impacts of each moisture mode will serve as actionable information which can be used by the stewards of La Vieja Misión in future interventive and preventive conservation.

List of Contents for Appendix A

Appendix I: Maps

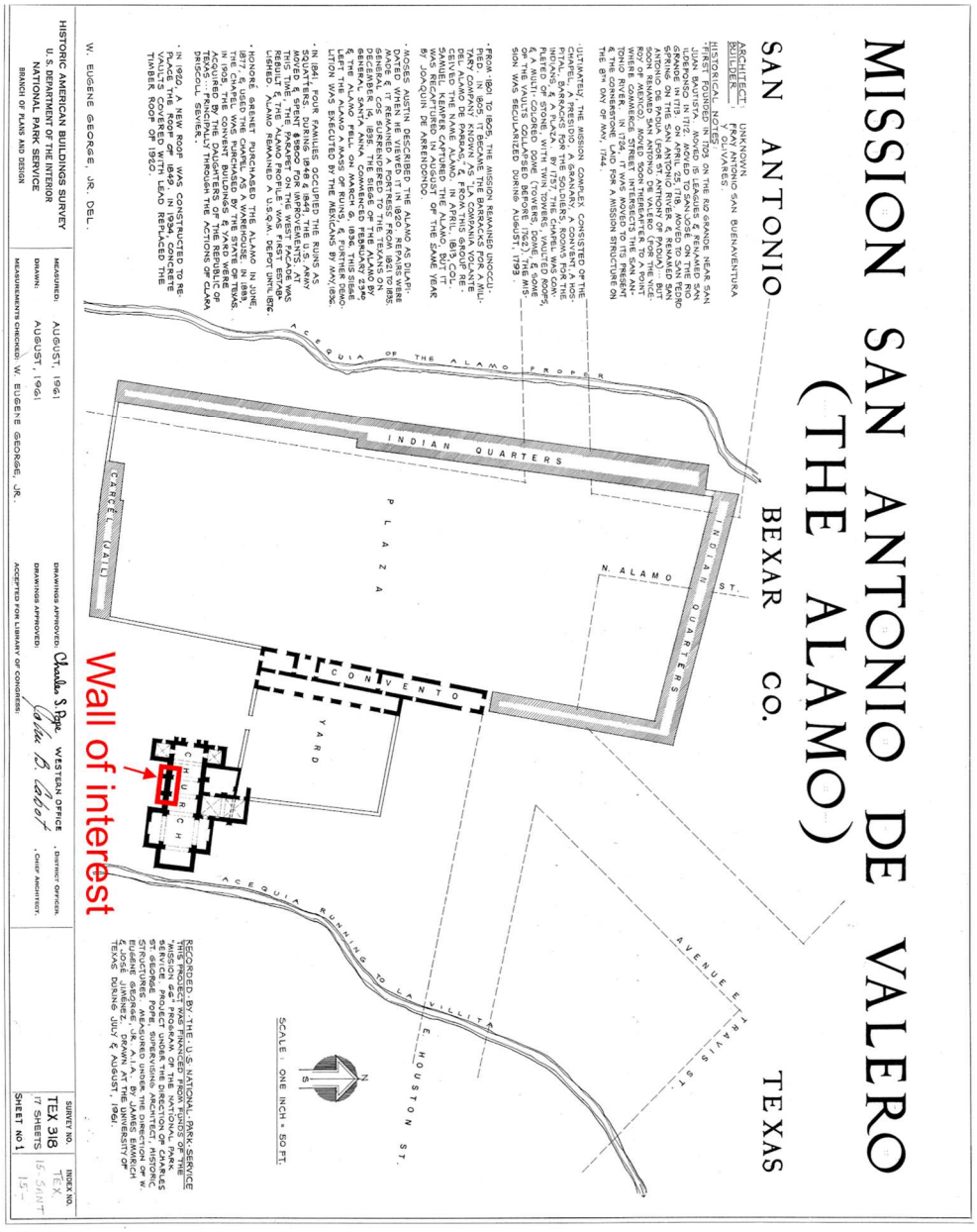

Figure I.1 Map indicating the southern wall of interest for this project in the context of the whole site.

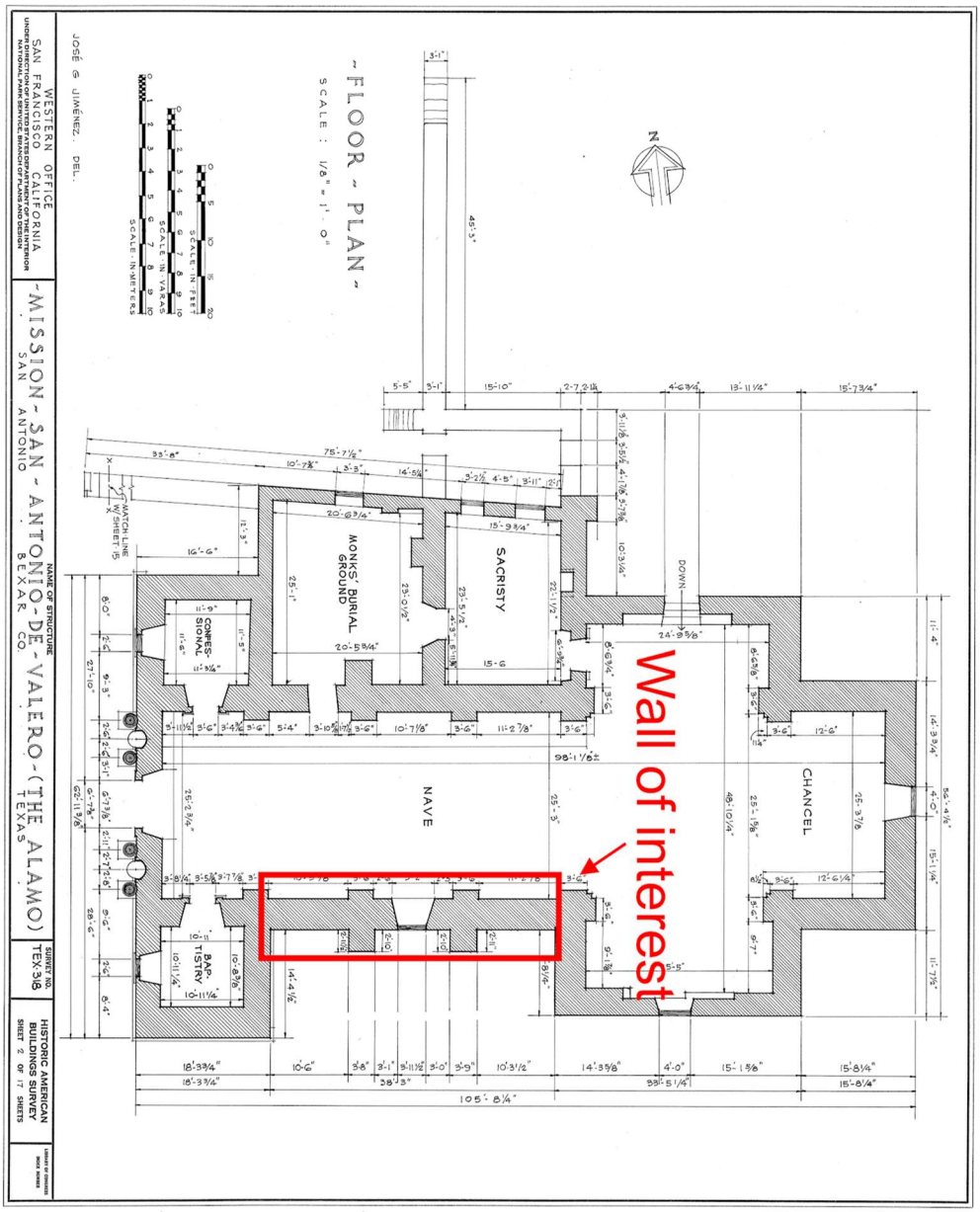

Figure I.2: Map indicating the southern wall of interest for this project in the context of the church.

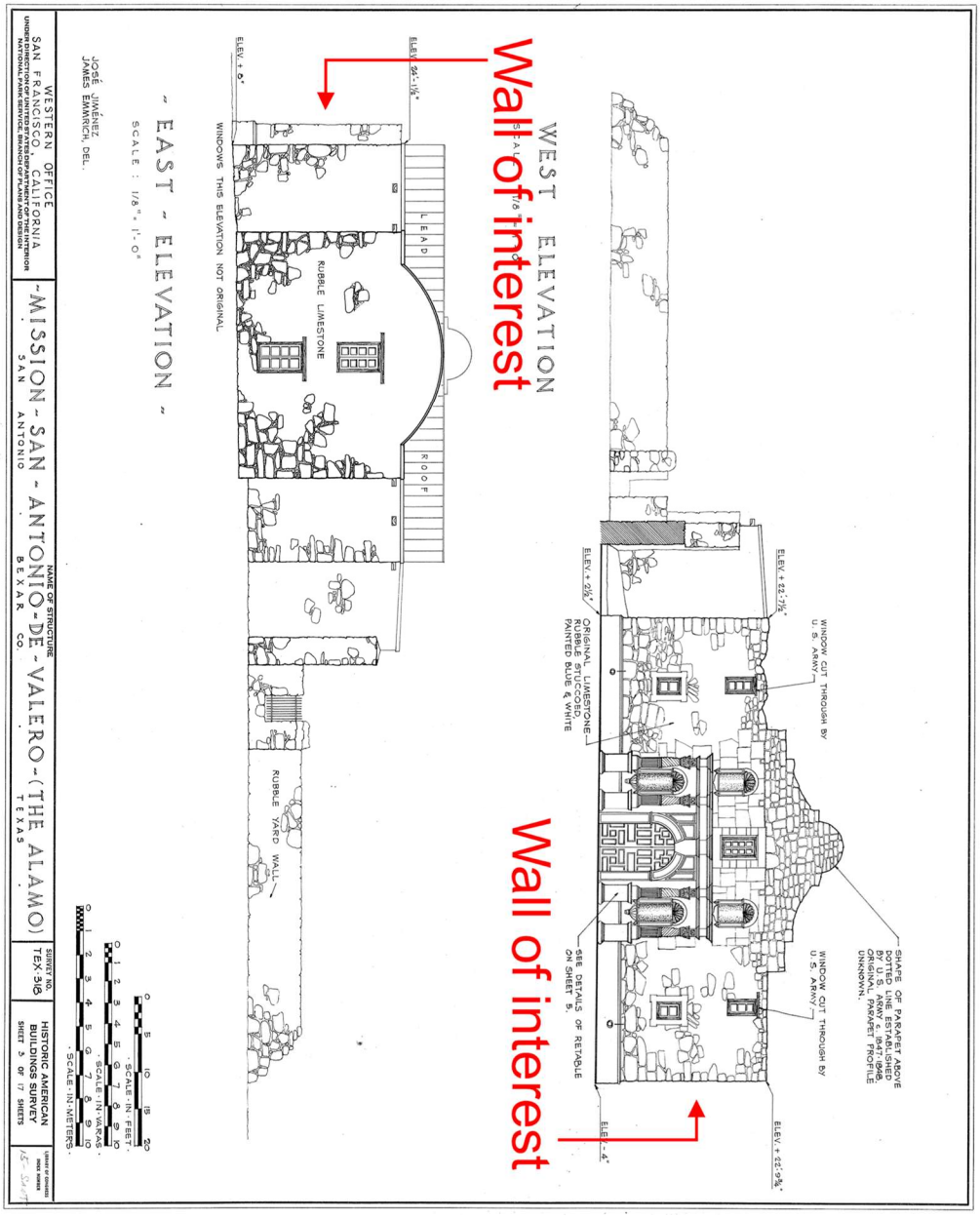

Figure I.3: Elevation map indicating where the wall of interest is located for this project in the context of the western and eastern elevations.

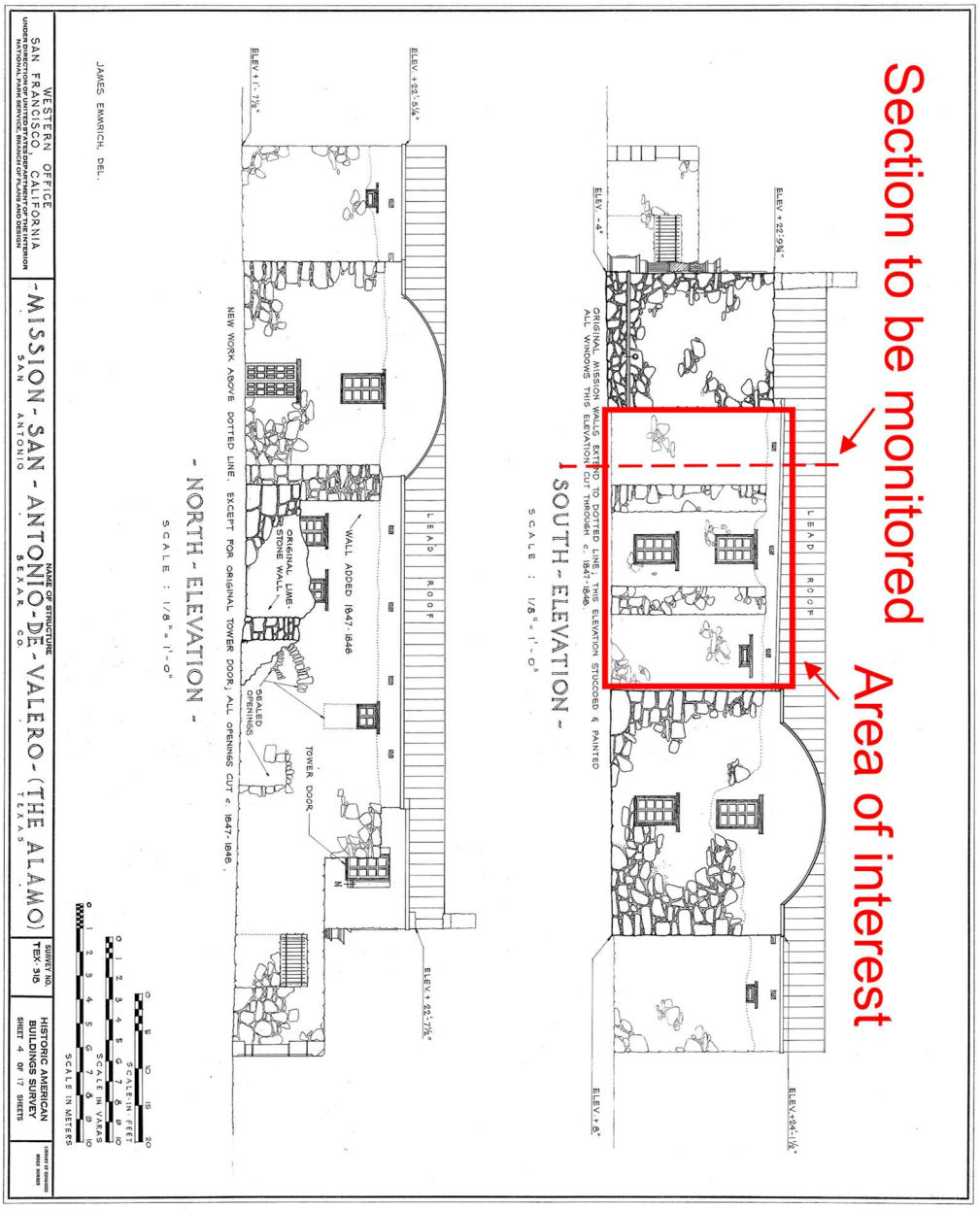

Figure I.4: Elevation map indicating where the area of interest and location to be monitored are located for this project in the context of the exterior southern elevation.

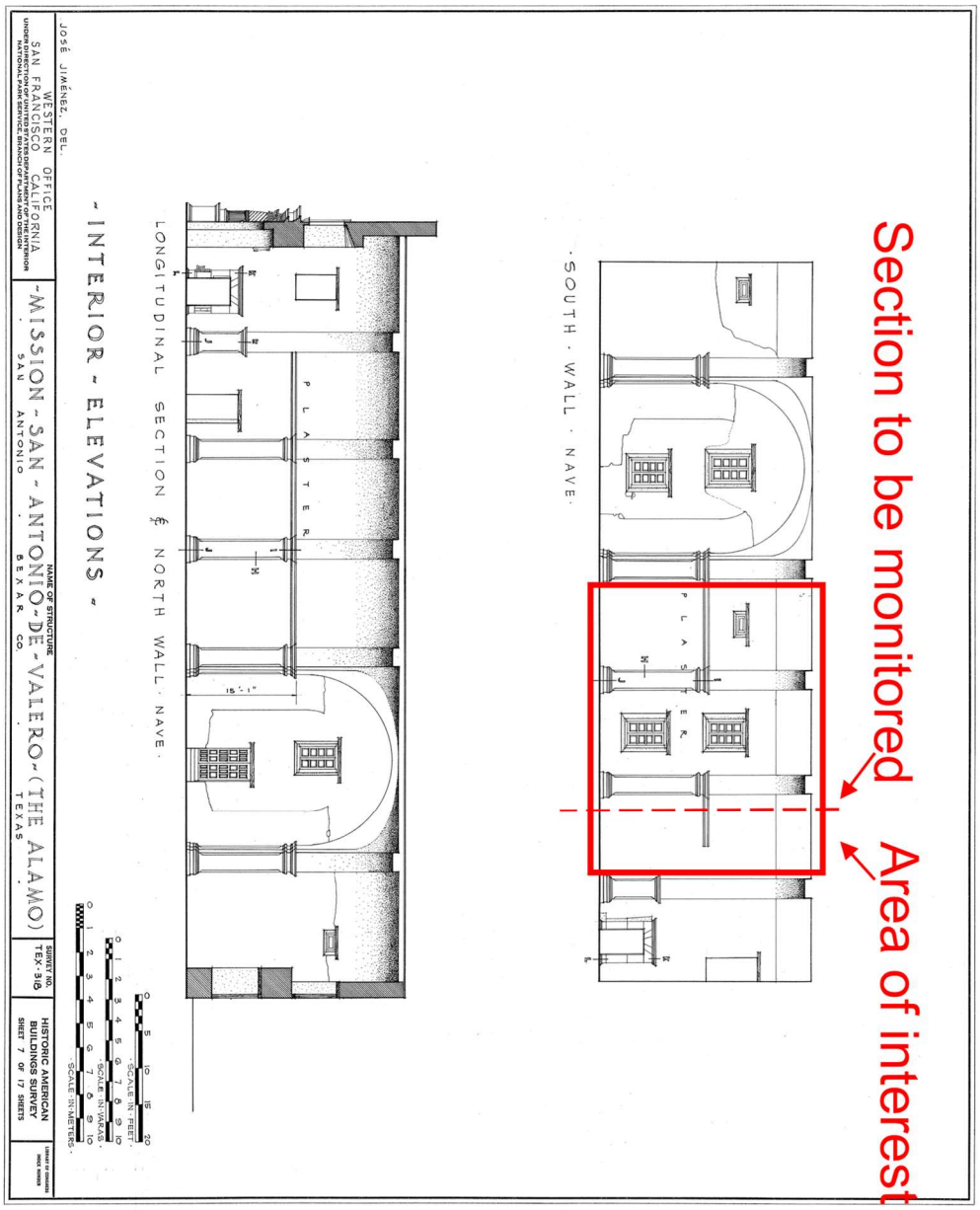

Figure I.5: Elevation map indicating where the area of interest and location to be monitored are located for this project in the context of the interior southern elevation.

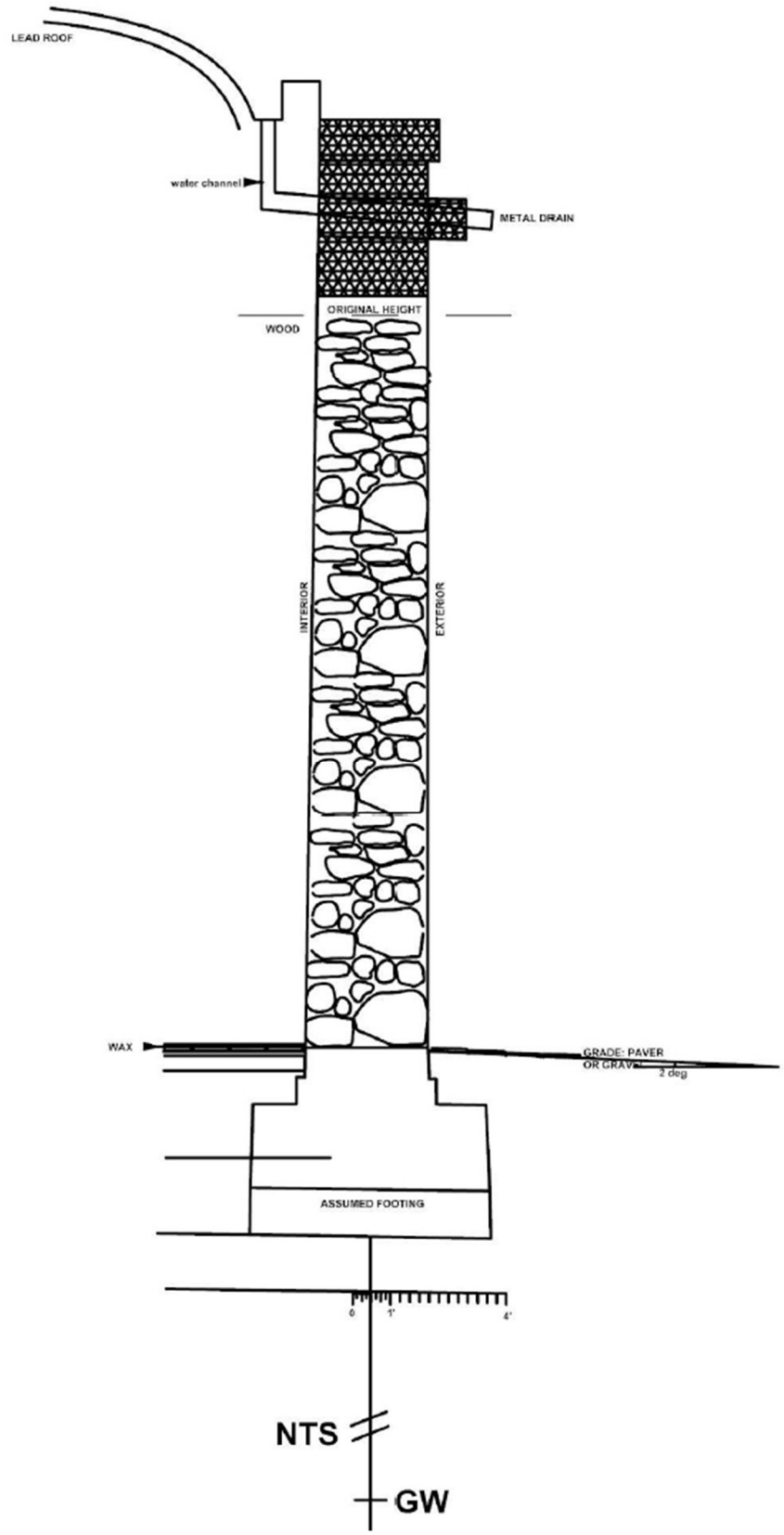

Figure I.6: Cross section of south wall.

Appendix II: Timeline

Figure II. 1 Timeline showing usage, structural changes, major climate events, historical events, and historical designations.

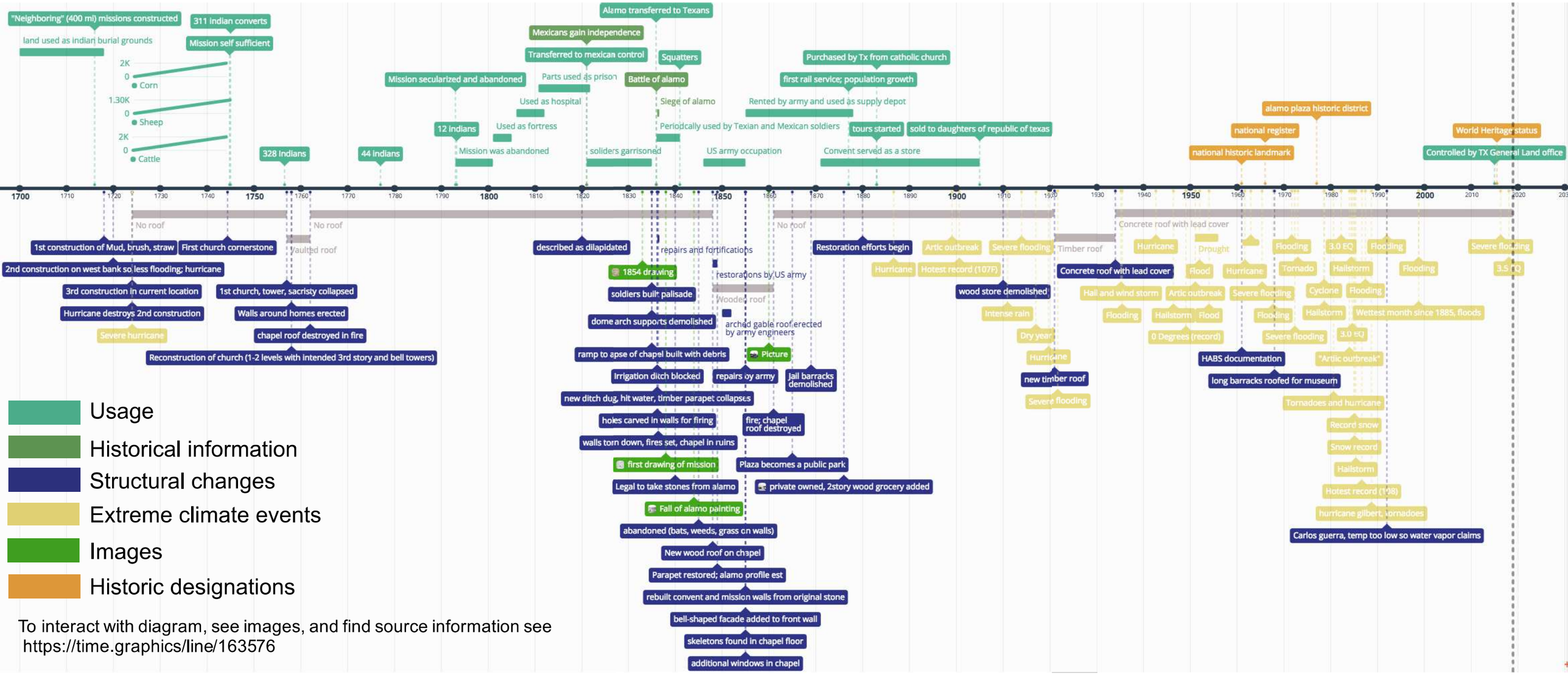

Usage

Historical information

Structural changes

Extreme climate events

Images

Historic designations

To interact with diagram, see images, and find source information see https://time.graphics/line/163576

APPENDIX III: Historic photographs

Figure III.1: Mid-1800's image showing exterior of the wooden roof[1]

INTERIOR OF ALAMO, WITH MODERN ROOF.—WHERE FINAL STAND WAS MADE.

[1] Source: https://rear-view-mirror.com/2017/03/16/past-and-present-the-alamo-san-antonio-texas/

Figure III.2: Wooden roof (mid 19th century)[2]

Figure III.3: 2015 Image showing the contemporary lead and concrete roof[3]

[2] Source: http://johnwayne-thealamo.com/forum/viewtopic.php?f=9&t=182&st=0&sk=t&sd=a&start=140

[3] Source: Edward A. Omelas, San Antonio Express-News

Appendix IV: Climate chart

Figure IV.1: Chart showing climate factors affecting the interior and exterior of the southern wall.

Exterior Climate Data for San Antonio, TX

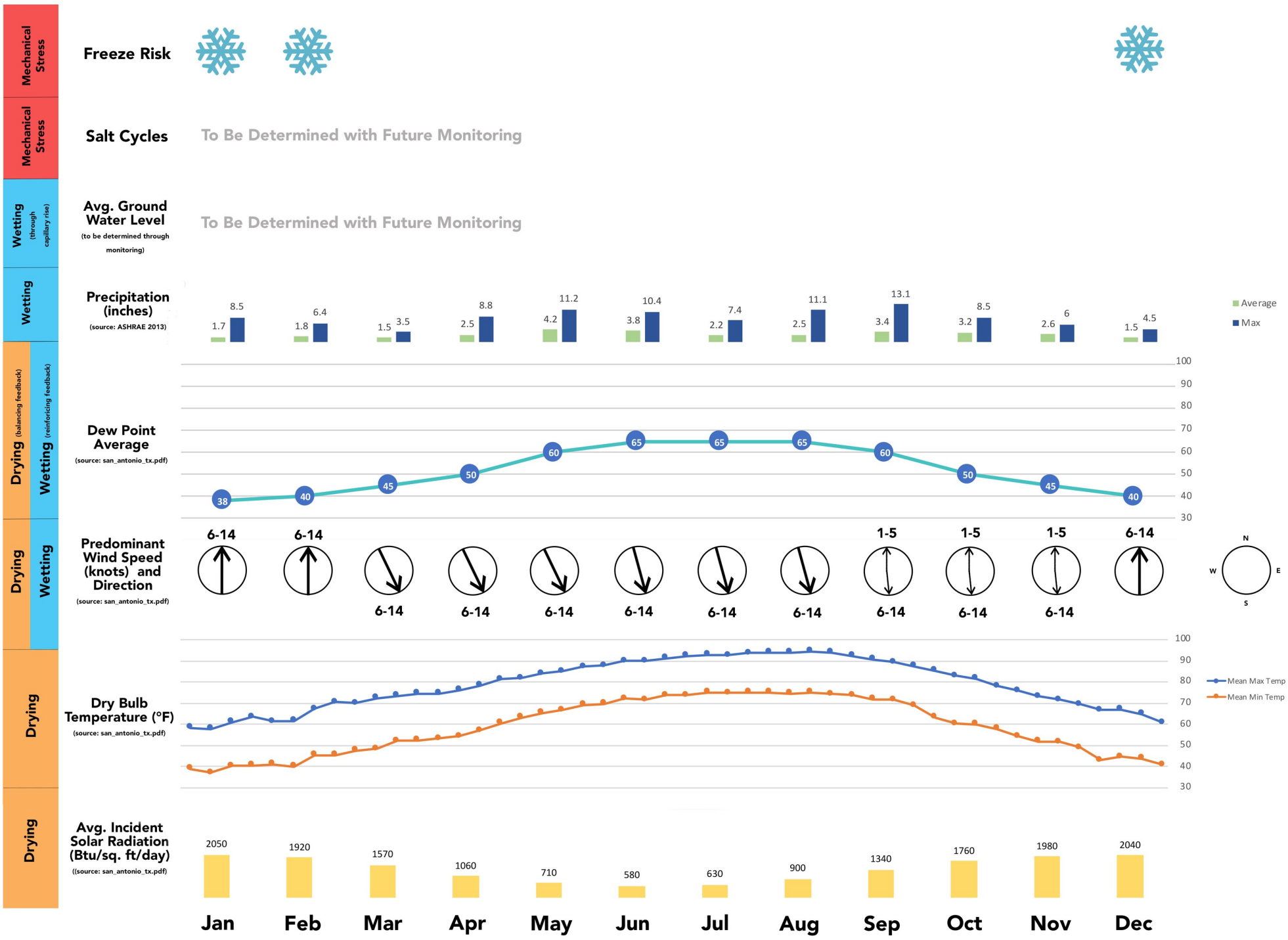

Interior Climate Data for La Vieja Misión

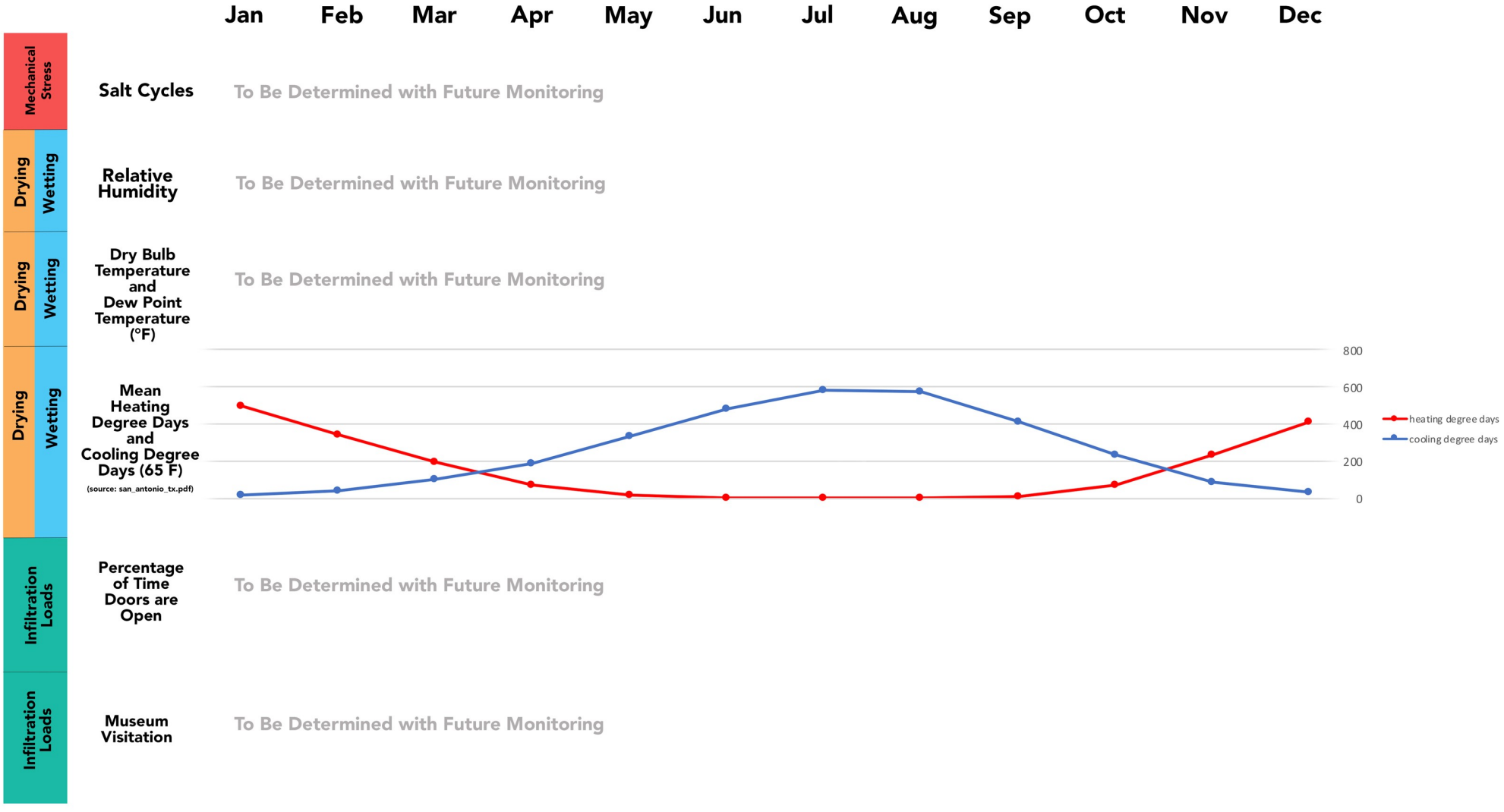

APPENDIX V: Stone identification

Types of Stone Identified by a stone conservator in La Vieja Misión and the Dominant Mode of Stone Deterioration: [1]

- A fluorescent white-cream dense chalk used in the carved elements of the west facade and interior, and randomly employed in the other walls;
- A fluorescent gray greenstone with dilatant clay inclusions; the distribution of the clay may be generalized or layered in many different directions. This stone is widely found through the church walls except the outer face of the north wall of the sacristy and the monk's burial room
- A high porous limestone without clays, having a sponge-like appearance and used in the outer face of the north wall of the sacristy and the monk's burial room and randomly scattered in the remaining walls

[1] Michael Henry, Class Instructions for Building Diagnostics, University of Pennsylvania, October 12, 2018.

Appendix VI: Systems diagrams

Figure VI.1: Full systems diagram showing not only sources of moisture and drying on the southern wall but also sensor locations, the presence of salts, and the impacts of humans.

Figure VI.2: Systems diagram showing the sources of moisture and drying on the southern wall

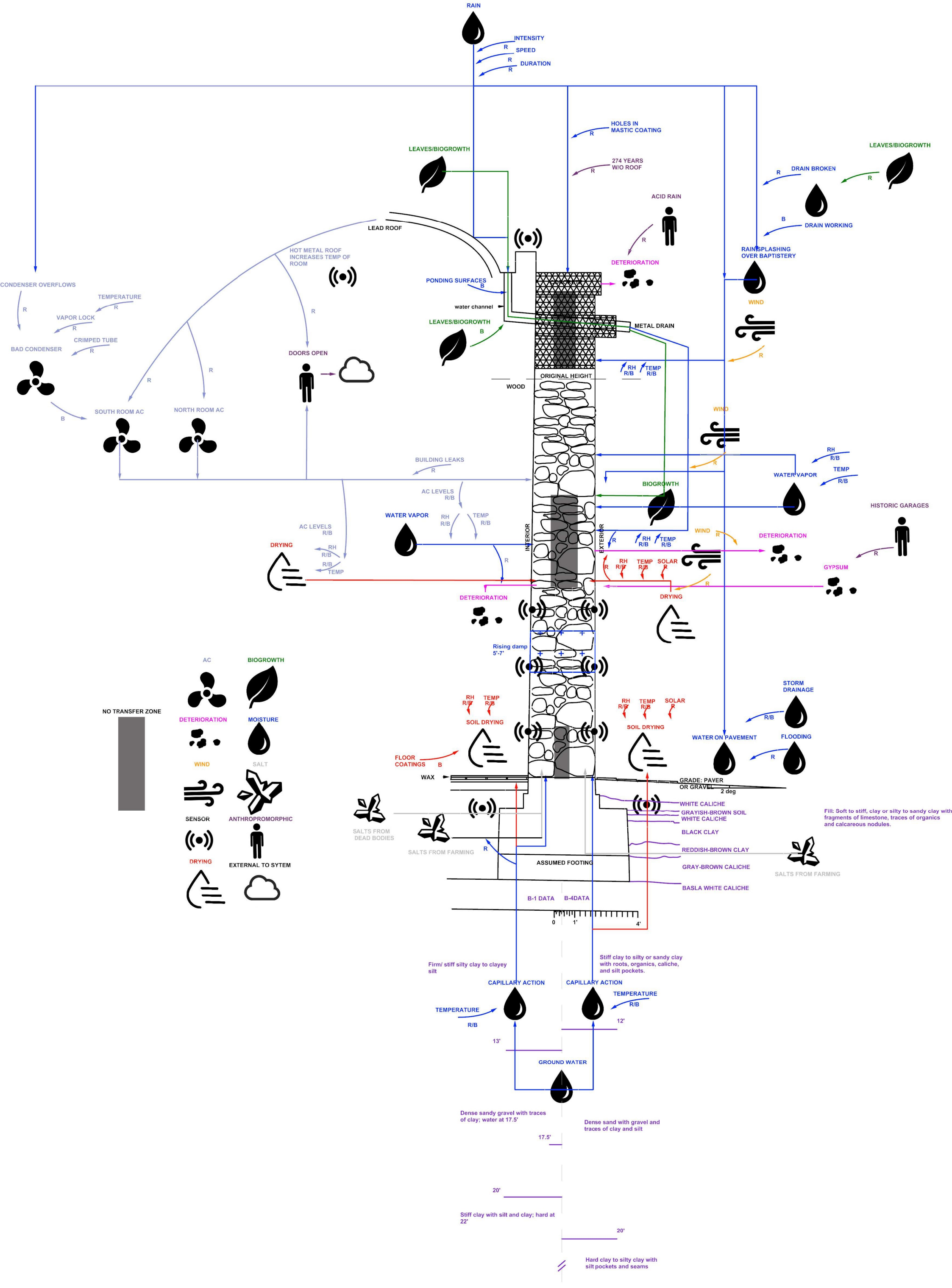
RAIN
INTENSITY
SPEED
DURATION
HOLES IN MASTIC COATING
274 YEARS W/O ROOF
LEAVES/BIOGROWTH
DRAIN BROKEN
DRAIN WORKING
ACID RAIN
LEAD ROOF
HOT METAL ROOF INCREASES TEMP OF ROOM
DETERIORATION
RAIN SPLASHING OVER BAPTISTERY
WIND
CONDENSER OVERFLOWS
TEMPERATURE
VAPOR LOCK
CRIMPED TUBE
BAD CONDENSER
PONDING SURFACES
CONCRETE
water channel
METAL DRAIN
DOORS OPEN
RH R/B
TEMP R/B
ORIGINAL HEIGHT
WOOD
SOUTH ROOM AC
NORTH ROOM AC
BUILDING LEAKS
AC LEVELS R/B
WATER VAPOR
BIOGROWTH
HISTORIC GARAGES
INTERIOR
EXTERIOR
DRYING
SOLAR R
GYPSUM
Rising damp 5'-7'
SOIL DRYING
STORM DRAINAGE
WATER ON PAVEMENT
FLOODING
FLOOR COATINGS
WAX
GRADE: PAVER OR GRAVEL
2 deg
WHITE CALICHE
GRAYISH-BROWN SOIL
WHITE CALICHE
BLACK CLAY
REDDISH-BROWN CLAY
GRAY-BROWN CALICHE
BASLA WHITE CALICHE
SALTS FROM DEAD BODIES
SALTS FROM FARMING
ASSUMED FOOTING
B-1 DATA
B-4DATA
0
1'
4'
Fill: Soft to stiff, clay or silty to sandy clay with fragments of limestone, traces of organics and calcareous nodules.
Firm/ stiff silty clay to clayey silt
Stiff clay to silty or sandy clay with roots, organics, caliche, and silt pockets.
CAPILLARY ACTION
TEMPERATURE
R/B
12'
13'
GROUND WATER
Dense sandy gravel with traces of clay; water at 17.5'
Dense sand with gravel and traces of clay and silt
17.5'
20'
Stiff clay with silt and clay; hard at 22'
Hard clay to silty clay with silt pockets and seams
NO TRANSFER ZONE
AC
BIOGROWTH
DETERIORATION
MOISTURE
WIND
SALT
SENSOR
ANTHROPROMORPHIC
DRYING
EXTERNAL TO SYTEM

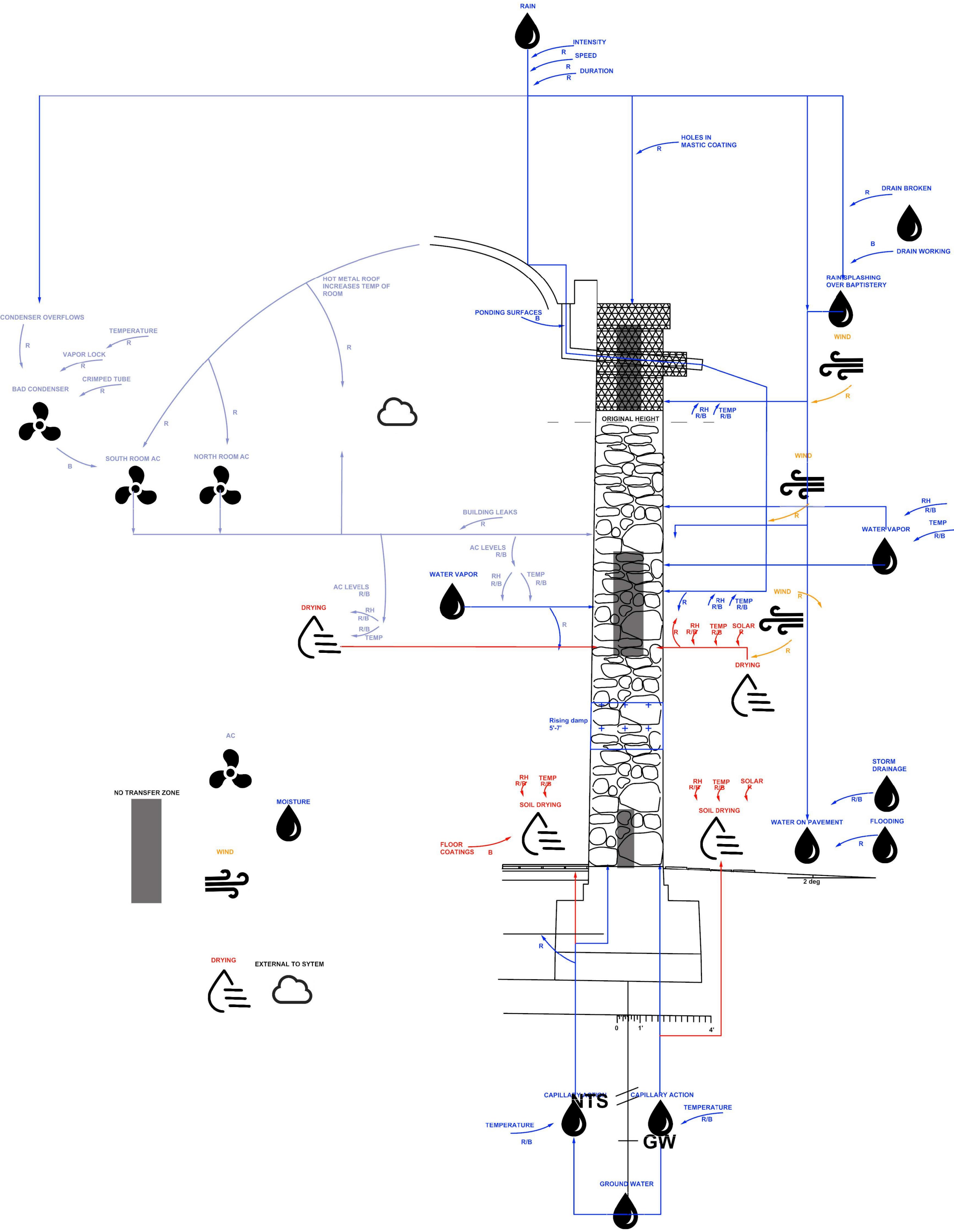
RAIN
INTENSITY
R
SPEED
R
DURATION
R
HOLES IN
MASTIC COATING
R
DRAIN BROKEN
R
B
DRAIN WORKING
RAIN SPLASHING
OVER BAPTISTERY
WIND
R
CONDENSER OVERFLOWS
R
TEMPERATURE
R
VAPOR LOCK
R
CRIMPED TUBE
R
BAD CONDENSER
B
SOUTH ROOM AC
NORTH ROOM AC
HOT METAL ROOF
INCREASES TEMP OF
ROOM
R
R
R
PONDING SURFACES
B
RH
R/B
TEMP
R/B
ORIGINAL HEIGHT
WIND
R
RH
R/B
TEMP
R/B
WATER VAPOR
BUILDING LEAKS
R
AC LEVELS
R/B
WATER VAPOR
RH
R/B
TEMP
R/B
AC LEVELS
R/B
DRYING
RH
R/B
R/B
TEMP
R
R
RH
R/B
TEMP
R/B
WIND
R
R
RH
R/B
TEMP
R/B
SOLAR
R
R
DRYING
Rising damp
5'-7'
AC
NO TRANSFER ZONE
MOISTURE
WIND
RH
R/B
TEMP
R/B
SOIL DRYING
FLOOR
COATINGS
B
RH
R/B
TEMP
R/B
SOLAR
R
SOIL DRYING
STORM
DRAINAGE
R/B
WATER ON PAVEMENT
FLOODING
R
2 deg
R
0
1'
4'
DRYING
EXTERNAL TO SYTEM
CAPILLARY ACTION
CAPILLARY ACTION
TEMPERATURE
R/B
TEMPERATURE
R/B
NTS
GW
GROUND WATER

Appendix VII: Sensor matrix

Figure VII.1: Matrix of recommended sensors, manufacture, shortened web address, accuracy, resolution, drift, and battery life.

Parameter	Manufa	Sensor name	Catalog number	Web address	Location	Accuracy	Resolution	Measurement range	Drift	Battery life
RH wall and air	Onset	12-bit Temperature/Relative Humidity (2m cable) Smart Sensor	# S-THB-M002	https://goo.gl/ZzqAzW	southern wall interior; southern wall exterior; interior wall; southern roof interior; southern roof exterior	Temp: 0.38°F from 32° to 122°F RH: +/- 2.5% from 10% to 90% RH	Temp: 0.04°F at 77°F RH: 0.1% RH	Temp: 40°F to 167°F RH: 0-100% RH at --40° to 167°F	Temp: <0.18°F/ year RH: < 1% per year	n/a
Soil moisture	Onset	EC5 Soil Moisture Smart Sensor	# S-SMC-M005	https://goo.gl/wqiPzM	southern wall exterior; southern wall interior	±0.031 m^3/m^3 (±3.1%)	0.0007 m^3/m^3	0 to 0.550(m^3/m^3)	not available	n/a
Rain amount and intensity	Onset	HOBO Rain Gauge Data Logger	# RG3	https://goo.gl/N3zCvQ	southern roof	±1.0%	0.01 in.	max 5 in. per hour	not available	1 year
Solar gains	Onset	Solar Radiation (Silicon Pyranometer) Smart Sensor	# S-LIB-M003	https://goo.gl/jXDt5m	southern roof	±10 W/m2 or ±5%	1.25 W/m2	0 to 1280 W/m2	<±2% per year	n/a
Wind speed and direction	Onset	Wind Speed and Direction Set Smart Sensor	# S-WSET-B	https://goo.gl/XMyt9d	southern roof	Speed: 2.4 mph or ± 4% of reading Direction: ± 5 degrees	Speed: 1.1 mph Direction: 1.4 degrees	Speed: 0 to 170 mph Direction: 0 to 355 degrees	not available	n/a
Groundwater level	Onset	HOBO Bluetooth Low Energy Water Level Data Logger	# MX2001-04	https://goo.gl/FAYSRw	southern wall exterior	0.015 ft	0.007 ft	0 to 30 ft	not available	1 year
Door opening	Onset	HOBO Extended Memory State Data Logger	# UX90-001M	https://goo.gl/eJkUcz	entrance door; exit door	time accuracy = +1 min/month	1 event	0-1Hz	not available	1 year
Condeser and AC unit state	Onset	HOBO Extended Memory Motor On/Off Data Logger	# UX90-004M	https://goo.gl/m7J4ne	see Figure 10	time accuracy = +1 min/month	1 event	0 to 2.5 V DC	not available	1 year
Salinity	Onset	HOBO Salt Water Conductivity/Salinity Data Logger	# U24-002-C	https://goo.gl/RcECn3	southern wall interior; southern wall exterior	3% of reading or 50 µS/cm	not available	100 to 10,000 uS/cm	Up to 12%/month	3 years
Ph of soil and rain	Onset	HOBO Bluetooth Low Energy pH and Temperature Data Logger	# MX2501	https://goo.gl/YpFAeS	southern wall interior; southern wall exterior; southern roof exterior	±0.10 pH units	0.01 pH	2.00 to 12.00 pH	not available	1 year
Data logger	Onset	HOBO RX3000 Remote Monitoring Station Data Logger	# RX3000	https://goo.gl/q6TCr5	see Figure 10	time: ±8 seconds per month	not available	operating range: -40° to 140°F	not available	1 year
Rising damp height	FLIR	FLIR E53	FLIRE53	https://goo.gl/LNc4aF	southern wall interior; southern wall exterior	±3.6°F or ±2% of reading	240 × 180 (43,200 pixels)	spectral range: 7.5 - 14.0 µm	not available	2.5 hours

APPENDIX VIII: Soil Profiles

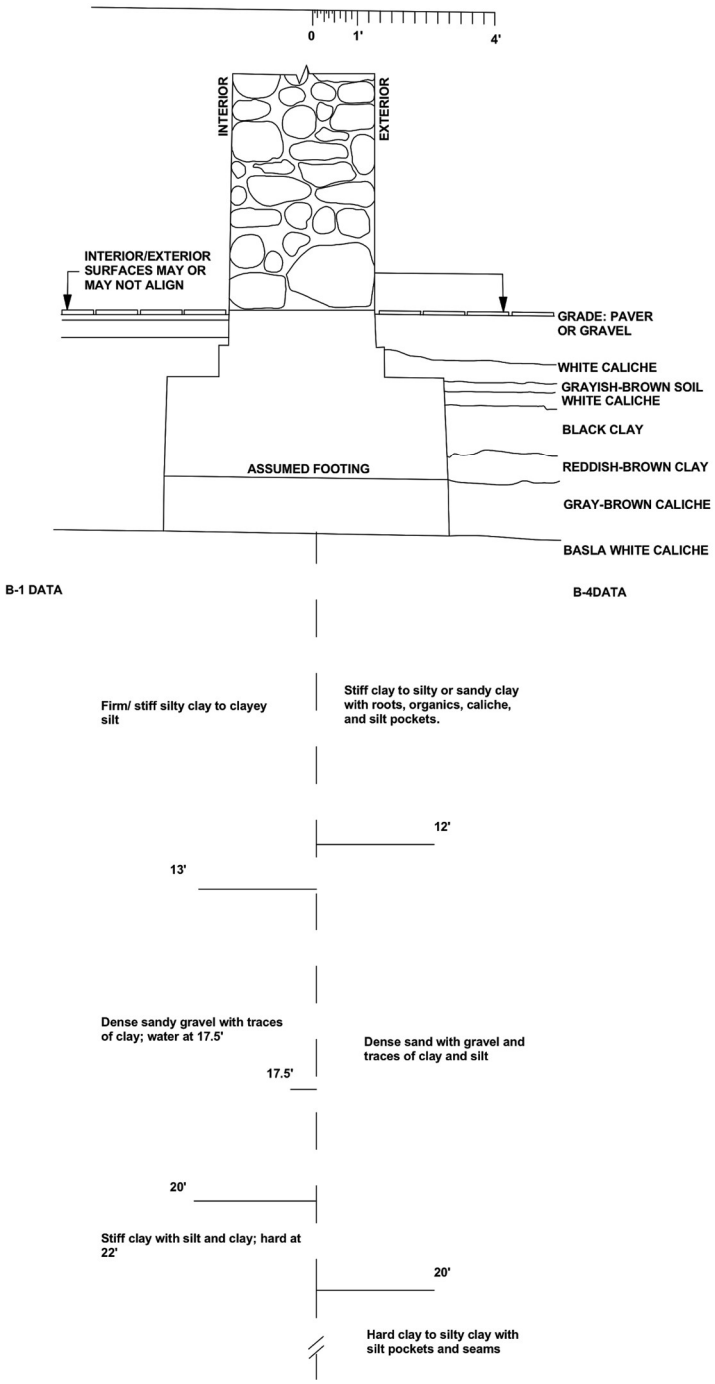

Figure VIII.1: Diagram of soil types and water levels. Soil strata close to the surface were determined by archaeology whereas the deeper soil identification is a composite from two testing sites near the south wall[1]. Those locations can be seen in Figure VIII.2.

[1] "Soil and Groundwater Study Progress Report No. 1, The Alamo Shrine" Raba-Kistner Consultants, Inc. April 18, 1984

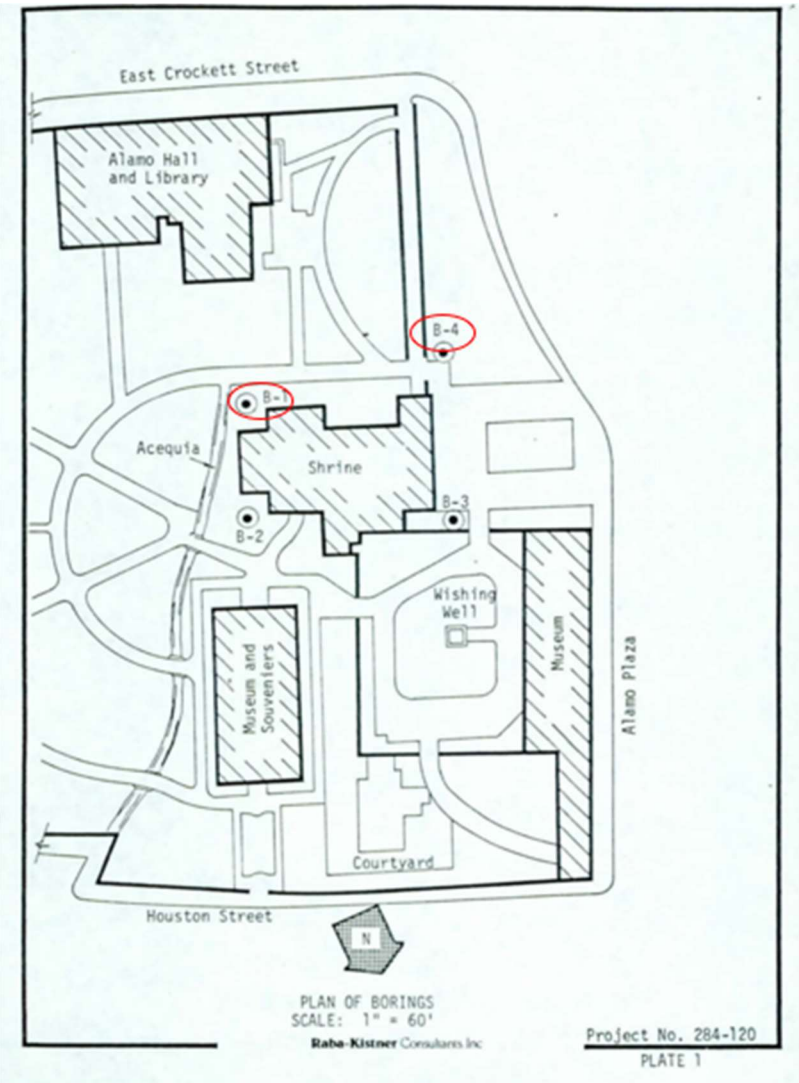

Figure VIII.2: Locations of soil testing nearest the south wall of the shrine.[2]

[2] "Soil and Groundwater Study Progress Report No. 1, The Alamo Shrine" Raba-Kistner Consultants, Inc. April 18, 1984

Appendix IX: Data management calculations

IX. 1 RX3000

First the allowable number of measurements per channel should be calculated.

$$\frac{43000\ measurements}{1\ data\ logger} \times \frac{1\ data\ logger}{15\ channels} = \frac{2866\ measurements}{1\ chann} \quad \text{Eq(IX.1)}$$

If measurements were recorded every 20 minutes for a year, how many measurements per channel would be needed?

$$\frac{1\ measurement}{20\ minutes} \times \frac{60\ minutes}{1\ hour} \times \frac{24\ hou}{1\ day} \times \frac{365\ days}{1\ year} = \frac{26280\ measurements}{1\ yea} \quad \text{Eq(IX.2)}$$

If data delivery is conducted once a month, how many measurements per month would that require?

$$\frac{26280\ measurements}{1\ year} \times \frac{1\ year}{12\ hours} = \frac{2190\ measurements}{1\ month} \quad \text{Eq(IX.3)}$$

Since the allowable number of measurements is greater than the required amount, this data retrieval schedule is permissible.

IX. 2 HOBO Extended Memory State Data Logger

The current visitation rates are 1.6 million visitors per year and this is expected to increase for 2019. Therefore an estimate of 2 million is taken for the number of visitors in 2019. If there are 2 million visitors, how many discrete data sessions would be required?

$$\frac{2000000\ measurements}{1\ year} \times \frac{1\ data\ logger}{340000\ measurements} = \frac{5.88\ data\ logs}{1\ year} \quad \text{Eq(IX.4)}$$

Since this would be too frequent to make site visits, a method involving extrapolation is suggested. If the total number of guests in a year is 2 million and the peak months for visitation are July and August, then a normal distribution can be defined for the period of 2019. The equation to describe this curve would be as follows:

$$Y = P(t) \times (2\ million - 365c) + c \quad \text{Eq(IX.5)}$$

Where P is a probability function that defines the normal distribution and c is a baseline of expected visitation (here assumed to be 100,000 people per month at a minimum. In Matlab, the probability function was assumed to be a normal distribution with a mean of 7 (this corresponds to the month of July) and a standard deviation of 3. To ensure that this equation approximates a normal distribution of visitation over a year, the integral under the curve can be taken. As it is two million, this equation does in fact represent a normal distribution of visitors.

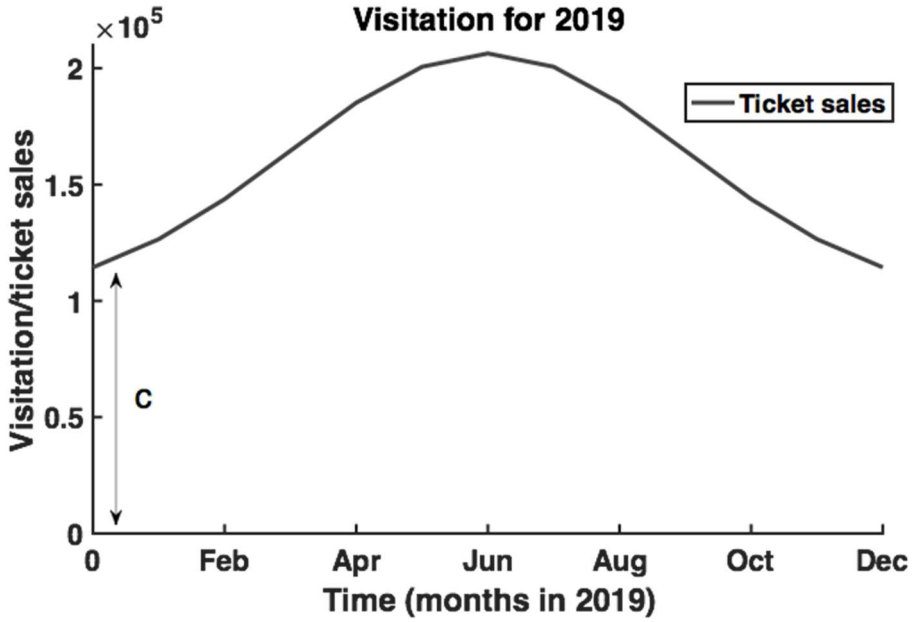

Figure IX.1: Illustration of the projected normal distribution of visitors during 2019.

As only 346,795 measurements can be recorded with this data logger, it has been suggested that the logger is turned on in January and run through mid-March. Then it should be run again in July through August. The integral under the curve for these specific ranges yields is 346,000 measurements which is acceptable for this logger.

IX. 3 HOBO Salt Water Conductivity/Salinity Data Logger

This data logger can hold 18500 measurements, therefore an appropriate logging interval needed to be calculated.

$$\frac{18500\ measurements}{1\ year} \times \frac{1\ year}{365\ days} \times \frac{1\ day}{24\ hours} = \frac{2.11\ measures}{1\ hour} \qquad \text{Eq(IX.6)}$$

Therefore a logging interval of 30 minutes is appropriate for this sensor

IX. 4 HOBO Bluetooth Low Energy pH and Temperature Data Logger

This data logger can hold 43300 measurements, therefore an appropriate logging interval needed to be calcualted.

$$\frac{43{,}300\ measurements}{1\ year} \times \frac{1\ year}{365\ days} \times \frac{1\ day}{24\ hours} = \frac{4.90\ measures}{1\ hour} \qquad \text{Eq(IX.7)}$$

Therefore a logging interval of 20 minutes is appropriate for this sensor.

IX. 5 HOBO Rain Gauge Data Logger

This data logger can accomodate for 16000 tips and it tips every 0.01" of rain. Therefore, if this was sufficient for a year needed to be calculated.

$$\frac{16000\ \ tips}{1\ data\ logger} \times \frac{0.01"\ rain}{1\ tip} = \frac{160\ "\ rain}{1\ data\ logger} \qquad \text{Eq(IX.8)}$$

According to previous climate data for this area, 31.0" of rain is the average and 50.8" would be the maximum in a year. Therefore, this data logger is acceptable for this project.

Appendix X: Bibliography

Background Information:

"Annual Average Humidity in Texas." Current Results. Accessed December 16, 2018. https://www.currentresults.com/Weather/Texas/humidity-annual.php.

“Annual Texas Live Oak Leaf Drop,” Texas Plant Disease Diagnostic Lab, Texas A&M Agrilife Extension, accessed November 30, 2018, https://plantclinic.tamu.edu/2011/03/30/annual-texas-live-oak-leaf-drop/

Henry, Michael. 2018. Personal Communication. Meyerson Hall, University of Pennsylvania, Philadelphia, PA

Holmes, Chris. "Best Cell Phone Carriers and Coverage in San Antonio." WhistleOut. November 13, 2018. Accessed December 16, 2018. https://www.whistleout.com/CellPhones/Guides/Best-Plans-in-San-Antonio.

Library of Congress, Prints & Photographs Division, HABS, 1961

"National Centers for Environmental Information." National Climatic Data Center. Accessed December 16, 2018. https://www.ncdc.noaa.gov/.

Raba-Kistner Consultants, INC, *Soil and Groundwater Study Progress Report No. 1 The Alamo Shrine San Antonio, Texas*, technical report (1984).

“San Antonio Missions,” UNESCO Nomination to the World Heritage List by the United States of America, self published, 2014

“San Antonio de Valero Mission,” Texas State Historical Association, accessed November 19, 2018, https://tshaonline.org/handbook/online/articles/uqs08

Deterioration Problems:

Changgeng Peng and Chak K Chan, “The Water Cycles of Water-Soluble Organic Salts of Atmospheric Importance,” *Atmospheric Environment* 35, no. 7 (January 1, 2001): 1183–92, https://doi.org/10.1016/S1352-2310(00)00426-X.

Espinosa, Rosa; Lutz Franke, and Gernod Deckelmann, “Predicting Efflorescence and Subflorescences of Salts,” MRS Proceedings 1047 (January 2007), https://doi.org/10.1557/PROC-1047-Y04-03.

Florian, Mary-Lou E. 2002. *Fungal Facts: Solving fungal problems in heritage collections.* London, UK: Archetype Publications Ltd.

Lucero, Sarah. "Verify: Is Alkaline Water Healthier than Regular Tap Water?" KENS5. June 15, 2017. Accessed December 16, 2018. https://www.kens5.com/article/news/local/verify/verify-is-alkaline-water-healthier-than-regular-tap-water/449171086.

Odegaard, Nancy, Scott Carroll, and Werner S. Zimmt. 2000. *Material Characterization Tests for Objects of Art and Archaeology.* London: Archetype Publications Ltd.104, 124,108.

Watt, David. 2007. *Building Pathology.* Oxford: Blackwell Publishing Ltd.

Wheeler, George, stone conservation lecture, Winterthur/University of Delaware Program in Art Conservation, March 5, 2018

Measurement and Monitoring:

Alberta Agriculture and Forestry. "Soil Moisture and Temperature Consideration." Alberta Agriculture and Forestry. January 06, 2012. Accessed December 16, 2018. https://www1.agric.gov.ab.ca/$department/deptdocs.nsf/all/crop1272.

Barreira, R.m.s.f. Almeida, and J.m.p.q. Delgado, "Infrared Thermography for Assessing Moisture Related Phenomena in Building Components," Construction and Building Materials 110 (2016): , doi:10.1016/j.conbuildmat.2016.02.026.

Buck, S. "Searching for graves using geophysical technology: field tests with ground penetrating radar, magnetometry, and electrical resistivity." *Journal of Forensic Science* 48, no. 1 (2003): 1-7.

Campbell Scientific. "Solar Radiation." Campbell Scientific. Accessed December 16, 2018. https://s.campbellsci.com/documents/us/category-brochures/b_solar-radiation.pdf.

Harris, Tom. "Living with Caliche." My San Antonio. October 26, 2005. Accessed December 16, 2018. https://blog.mysanantonio.com/waytogrow/2005/10/tom-harris-living-with-caliche/.

Met Office. "Fact Sheet No. 3 -- Water in the Atmosphere." *National Meteorological Library and Archive*, 2012. Accessed December 16, 2018.

Mboya, Hieronimi A., Cecil K. King'ondu, Karoli N. Njau, and Alex L. Mrema. 2017. "Measurement of Pozzolanic Activity Index of Scoria, Pumice, and Rice Husk Ash as Potential Supplementary Cementitious Materials for Portland Cement." Research article. Advances in Civil Engineering. 2017. https://doi.org/10.1155/2017/6952645.

Miyamoto, S. "Supplement to Diagnosis and Management of Salinity Problems in Irrigated Pecan Production: Salt Leaching." *Texas Water Resources Institute Technical Report No. 387A*, 2010. Accessed December 16, 2018.

"Northeast Region Certified Crop Adviser (NRCCA) Study Resources." Certified Crop Advisor Study Resources (Northeast Region). Accessed December 16, 2018. https://nrcca.cals.cornell.edu/soil/CA2/CA0212.1-3.php.

"Official Aquifer Level & Statistics." San Antonio Water System. Accessed December 16, 2018. https://www.saws.org/Your_Water/aquifer/.

Rosina, Elisabetta and Nicola Ludwig, "Optimal Thermographic Procedures for Moisture Analysis in Building Materials," Diagnostic Imaging Technologies and Industrial Applications, September 10, 1999, , doi:10.1117/12.361015.

Ruffell, Alastair, Alan McCabe, Colm Donnelly, and Brian Sloan. "Location and assessment of an historic (150–160 years old) mass grave using geographic and ground penetrating radar investigation, NW Ireland." *Journal of forensic sciences* 54, no. 2 (2009): 382-394.

Unterberger, R. R. "Ground penetrating radar finds disturbed earth over burials." In *Fourth International Conference on Ground Penetrating Radar*. 1992.